Nano-grinding zinc oxide for electronic applications

by

Sahil Dawka
Bachelor of Technology, Amity University, 2015

A Project Report Submitted in Partial Fulfillment of the
Requirements for the Degree of

MASTER OF ENGINEERING

in the Department of Electrical & Computer Engineering

© Sahil Dawka, 2019
University of Victoria

All rights reserved. This thesis may not be reproduced in whole or in part, by photocopy or other means, without the permission of the author.

Supervisory Committee

Nano-grinding zinc oxide for electronic applications

by

Sahil Dawka

Bachelor of Technology, Amity University, 2015

Supervisory Committee

Dr. Christo Papadopoulos, Supervisor
Department of Electrical & Computer Engineering

Dr. Tao Lu, Departmental Member
Department of Electrical & Computer Engineering

Abstract

Planetary ball milling (PBM) is a type of high energy ball milling, which is a top down technique for fabricating nanomaterials. PBM was used to fabricate zinc oxide nanoparticles by nano-grinding, followed by thin film device fabrication via drop casting, and characterization of electrical properties such as conductance and photosensitivity. Grinding parameters such as speed were varied to produce different batches of material, and thermal treatment was carried out, to form films with different properties and an analysis of the effect of these factors was attempted. Increasing the grinding speed was found to generally reduce the value of conductance of the thin films. Zinc oxide was also milled with indium tin oxide in isopropyl alcohol, to attempt mechanochemical composite formation with the zinc oxide nanoparticles. The films of this material showed increased conductance and sensitivity to light. Some avenues of extending this work were suggested, including various device structures and fabrication techniques.

Contents

List of Tables

List of Figures

List of Acronyms

PBM - Planetary Ball Milling

ITRS - International Technology Roadmap for Semiconductors

MBE - Molecular Beam Epitaxy

PLD - Pulsed Layer Deposition

ZTO - Zinc Tin Oxide

ITO - Indium Tin Oxide

RAM - Random Access Memory

SRAM - Static RAM

DRAM - Dynamic RAM

FPGA - Field Programmable Gate Array

MSM - Metal-Semiconductor-Metal

SCS - Semiconductor Characterization System

EG - Ethylene Glycol

IPA - Isopropyl Alcohol

Acknowledgements

I would like to thank my supervisor Dr. Chris for his guidance throughout my degree, and for being a reliable source of motivation, knowledge, and wisdom.

I would also like to express gratitude towards my colleagues and friends, including Raju and Anusha, whose help and moral support was invaluable.

Finally I'd like to thank my family for their generous support and patience which has enabled me every opportunity.

Chapter 1

Introduction

1.1 Motivation

Broadly speaking, there are two main categories of nanofabrication - top down and bottom up. Bottom up approaches utilize naturally occuring mechanisms such as self-assembly to achieve fabrication of desired nanostructures, where we start with molecular building blocks, and forces at the molecular level result in desirable effects such as mass alignment or structural configurations. Top-down approaches in nanotechnology achieve nanoscale order or effects by starting with a macroscale material and having it undergo subtractive processes, such as electron beam lithography, or breaking down the material via chemical or physical means, such as etching or milling. Analogously, materials research can be broadly divided into two categories - application focused, when we aim to find an optimal material for a particular purpose, and material focused, when the aim is to fabricate modified materials or novel combinations thereof, study their properties, and later adapt them to various potential applications. The application focused way is useful when there is a very particular pressing problem to solve, and there are multiple candidates to consider for the solution. The material focused research method is the way to generate knowledge of those candidates. Other major advantages of the materials focused research method are that it is less prone to confirmation bias, and data generated via such exploratory research retains its relevance and potential even after some applications have been found.

Here we fabricate zinc oxide thin films via planetary ball milling and study their electronic properties.

While the synthesis route is a top down approach, there is also a bottom up component of the nanoscale defects of individual particles contributing to the overall behaviour of devices fabricated in this work. There are many facts that make zinc oxide an interesting material, which are listed in the following chapter. We are measuring its electronic properties because there are many challenges in the industry today that do not have clear cut candidate solutions. Many existing applications are also ripe for reinvention, such as existing devices that can be redesigned for saving space or expanding efficiencies, with the help of better materials.

It is now widely accepted that Moore's Law will not hold for much longer [1]. While we aim to shrink current technologies, to achieve ever smaller space and energy consumption, we come across fundamental problems. Besides the difficulties in fabricating structures at such small length scales in a controlled manner, there is another issue. In contemporary electronic processors, information is represented by the presence/absence of charge, and computation is performed via control over the flow of the charge carriers. This control is achieved by using potential barriers and conductive paths to form circuit paths that represent different computations. Problems arise when the feature sizes approach mere multiples of the De-Broglie wavelengths of the particles we are manipulating to carry out computations. When the potential barriers used to contain the electrons become too thin, there is a considerable probability that the electrons 'leak' out of their designated space. Thus the overall electron flow (and by consequence, the overall computational circuit state) becomes unpredictable to such a degree that error correcting codes and redundancy failsafes are not able to guarantee a good enough confidence bound on the output of the system [2].

Furthermore, besides adding transistors to the circuit to obtain the ability to perform more logic operations, chip makers also aim to increase the frequency of the clock on the chip to obtain better performance. Microprocessors are very complex and can operate on multiple data streams concurrently. In order to maintain order, processors use a clock signal to synchronize data flow and manipulation steps across the entire circuit. Having a faster clock thus means more operations per unit time, and would require materials with high mobilities to be feasible, as the speed of any charge carrier in a medium is finite. Even with ballistic transport engineered to occur at as many places on the chip as possible, power is dissipated as heat at junctions and longer interconnects. Ten years or so ago, the industry decided

to level off on clock speed and focus on increasing the transistor count to obtain performance benefits. Today, consumer grade processors from AMD uses 7nm fabrication, which is almost at the limit of the smallest useful feature sizes technology can achieve.

In response to the challenge, the industry is going for two main approaches that are labelled "Beyond CMOS" and "More than Moore", as documented in the reports of the International Technology Roadmap for Semiconductors (ITRS) [1], which is a consortium of industry leaders in the semiconductor nanofabrication industry. Although at this point there is no clear alternate, it is self-evident that tomorrow's computational technology will have a fundamentally different architecture and utilize materials and phenomenon that are different from those in use today. As conventional fabrication technologies are beginning to stagnate when it comes to scaling, the industry requires new technologies that can scale well where today's NAND Flash, DRAM and SRAM cannot. At the same time, the new technologies should be compatible with existing technologies, even if they use radically dierent approaches. One such approach is to combine the logic and memory functions into a single device [3]. As our devices are electronic, the most useful property for this purpose is memristance. Among the active materials for such systems, transition metal oxides are said to be the most promising. Due to its availability, cost and variety of properties, we consider Zinc oxide to study.

1.2 Background

1.2.1 Method of Fabrication: Planetary Ball Milling

Ball milling is a well known technique for reducing particle size to the nanoscale, and in recent years it has also been adapted as a mechanochemical nanomaterial synthesis technique. Typically starting in powder form, a material is reduced to nanoscale dimensions by repeated fracturing from high energy impacts. Of the various types of ball mills such as mixer mills and stirred media mills, planetary ball milling (PBM) is preferred in the laboratory due to its moderate cost, efficient use of energy, and comparatively small size, comparatively simple usage procedures, and good cleanability [4].

The common planetary ball milling systems consist of two grinding jars on a planetary disk. The disk and the jars have their own axes of rotation, leading to high forces inside the jars due to centrifugal

forces of rotation and revolution. The material to be grinded is placed inside one or both jars, such that the weight is equally distributed. To this, solid milling balls are added. The impact of the milling balls/beads colliding against each other during operation of the PBM transfers energy to the material being grinded. The internal processes are complex and thus have to be assessed individually, depending on the synthesis materials and required particle sizes. The variables available to control in a PBM process for a given machine are the bead size, milling speed, milling time, the filling ratio, and whether or not a solvent is used. Depending on if a solvent is used or not, the process is referred to as wet milling and dry milling, respectively.

PBMs can be used for mechanical milling, when a uniform powder is processed into smaller particle sizes. They are also used for mixing, when different materials are mixed together in a grinding jar. The high energies of the impact can also result in the formation and breakage of chemical bonds, resulting in fundamental material changes such as alloying. In wet milling or colloidal grinding, at smaller particle sizes, high surface energies can cause radicalized solvent molecules to coat the particles, leading to functionalization of the material [5]. Varying the grinding parameters allows control over experimental conditions for nanoparticle synthesis. Thus we can find the optimal conditions to get the desired properties or distributions of grinded materials.

1.2.2 Material overview: Zinc oxide

Zinc Oxide (ZnO) is a II-VI semiconductor found in nature in the mineral zincite. However, as this often contains impurities, ZnO used for investigations is primarily synthesised material. Compared to other elements and compounds used for electronics, (such as Cd, Se, In, etc), Zn is more cost-effective to process, non-toxic, and abundant in the crust of our planet. This makes it a very suitable material for industrial applications, especially in nanostructured form [6]. Various forms of ZnO nanostructures are presented in figure 1.6. If the use of rare and scarce elements continues to proliferate in the industry, soon it will be more cost effective to obtain them from salvaged electronics instead of mining from the crust.

It is a wide band-gap semiconductor with a direct band gap of around 3.4eV [7], due to which pure ZnO is colorless and clear. In powdered form it has a white color that sometimes gets a tinge of yellow

after high energy grinding. Doping can increase or decrease the band-gap of ZnO to as low as 3.0 eV (with Cd) or as high as 4.0 eV (with Mg). Generally it is easier to synthesize n-type doped ZnO, but recently there have been more studies on fabricating p-type ZnO. This is promising as both types of materials are needed for constructing various heterostructures to harness quantum effects. The Hall mobility of electrons in ZnO thin films has been measured to be around $100 cm^2/Vs$ at room temperature. Hole mobilities at similar temperatures are found to be much lower, ranging from single digits to tens of cm^2V/s. The experimentally observed electrical properties of zinc oxide vary widely based on factors such as structure, crystallinity, adsorbates, defects, etc.

Molar mass	**Density**	**Melting point**	**Lattice constants**
81.406 g/mol [8]	$5.1 g/cm^3$ [8]	1974 ℃[8]	$a = 3.2495$ Å, $c = 5.2069$ Å [8]
Band gap (300K)	**Exciton energy**	**Electron mobility (300K)**	**Hole mobility (300K)**
$3.4eV$ [7]	$60meV$ [9]	$100 cm^2V^{-1}s^{-1}$ [9]	3-50$cm^2V^{-1}s^{-1}$ [9]

Table 1.1: Material properties of zinc oxide

Band and Crystal Structure

Although it has two main forms (figure 1.1) - hexagonal wurtzite and cubic zincblende, ZnO crystallizes preferentially in the wurtzite-type structure, especially since it is more stable at ambient temperatures.The zincblende form can be stabilized by growing ZnO on substrates with cubic lattice structure. ZnO also takes on the rocksalt structure at very high pressures. While the hexagonal unit cells are expected to have two lattice parameters of a and c ($c/a = \sqrt{8}/3$), the actual lattice of ZnO deviates slightly from the ideal lattice with $c/a = 1.602$ [10].

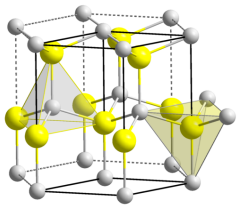

(a) Unit cell of wurtzite

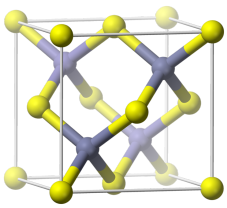

(b) Unit cell of zincblende

Figure 1.1: The two main crystal structures of ZnO

ZnO has a direct bandgap with the conduction band minimum and the valence band maximum located at $k = 0$ in the Brillouin zone. The conduction band of ZnO is predominantly s-like, while the

valence band is p-like. Spin–orbit splitting leads to a partial lifting of the valence band degeneracy: the six-fold degenerate valence band splits into a four-fold ($j = 3/2$) and a two-fold band ($j = 1/2$). Because of the lower symmetry of the wurtzite structure, the crystal field further lifts the valence band degeneracy. Thus crystal field splitting and spin–orbit coupling give rise to three two-fold degenerate valence bands from the valence band maximum, labelled A, B and C.

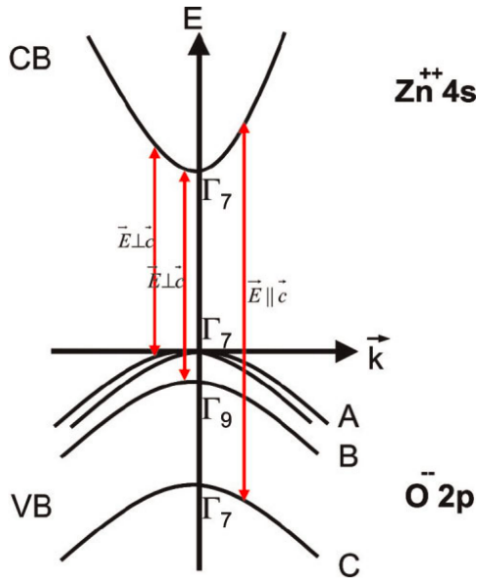

Figure 1.2: Schematic of the band structure of ZnO. A k-linear term possible for Γ_7 states for k perpendicular to c is shown schematically for the AΓ_7 valence band. The polarizations of the band-to-band transitions which are dipole allowed and do not involve a spin flip are indicated. [11]

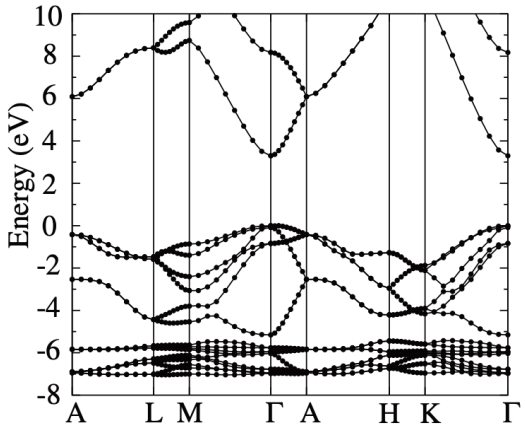

Figure 1.3: Calculated band structure of ZnO using the Heyd–Scuseria–Ernzerhof hybrid functional, and valence band maximum set to zero [12]

Defects

In nanostructured ZnO, the small length scales and large surface-to-volume ratio mean that surface defects play a pertinent role in controlling properties. Intrinsic defect levels occur in nominally undoped ZnO due to structural defects such as vacancies or interstitials in the crystal lattice, or dopant atoms such as hydrogen. The following is a summarization from reference [12] - Among native defects, oxygen vacancies are deep donors and cannot explain the observed spontaneous n-type conductivity in ZnO. Zinc interstitials are shallow donors, but are unlikely to be stable as isolated point defects because of high formation energies under n-type conditions and being fast diffusers. Zinc antisites are also shallow donors, inducing a large local lattice relaxation. They also have high formation energies in n-type samples. Zinc vacancies are deep acceptors and have low formation energies under n-type conditions, and are therefore thought to occur commonly as compensating defects in n-type samples. Oxygen interstitials have high formation energies and are not expected to exist natively in significant concentrations. Oxygen antisites have the highest formation energies among the acceptor-type native point defects. They are deep acceptors and also show large off-site displacements, in which the oxygen atom bonds chemically to only one of the oxygen nearest neighbors. Acceptor defects must be promoted to achieve p-type ZnO. The formation energies of different defect states are presented in figure 1.4.

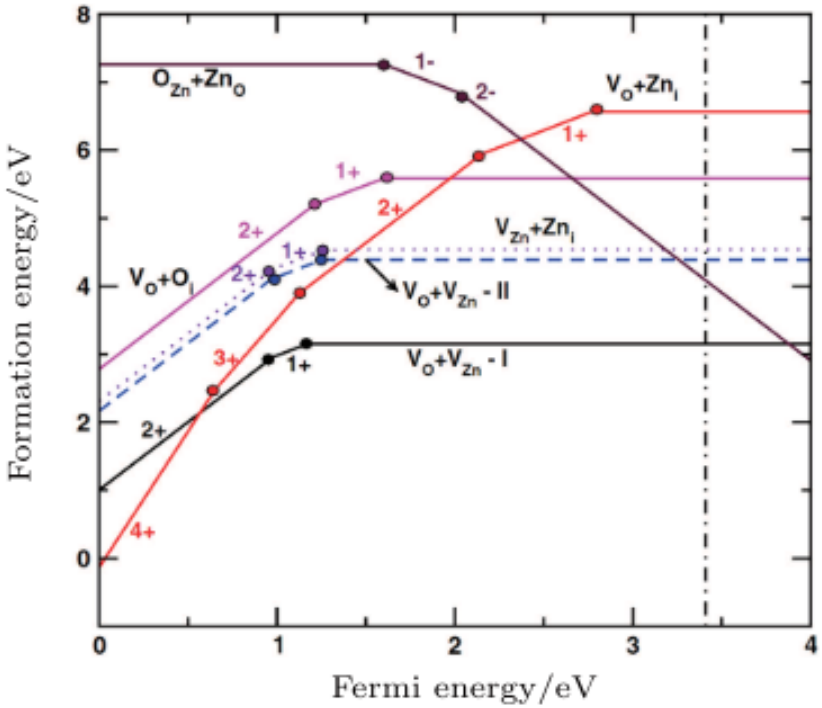

Figure 1.4: Formation energies of instrinsic defect states as a function of Fermi energy (under Zn-rich conditions) [13]

In the hexagonal close packed lattice, Zn atoms occupy half of the tetrahedral sites. Consequently, all the octahedral sites are empty. These can all serve as sites for ZnO to accommodate interstitial defects and extrinsic dopants. Therefore, ZnO has a lot of defect levels in the forbidden gap, both deep and shallow centres. Many of them can give rise to luminescence and absorption bands covering the spectral range from the ultra violet to the infra-red. It is still a matter of debate which types of defects dominates in native, undoped ZnO [14]. However, density functional calculations have given a better understanding, based on formation energies of various defects. The relative concentrations of the various defects depend strongly on temperature because of the different ionization energies. Surface defects contribute a lot to the electrical behaviour of ZnO, and this is sometimes used as an advantage, such as hydrogen annealed nanowires for nanoscale memory [15]. Other than point defects and the adsorption of moeties, zinc oxide, like other crystal structures, has grain boundaries where there is a break in periodicity of the lattice. The surface defects of ZnO also change based on the orientation of the terminal surface. Since it has ionic character and is not centro symmetric in wurtzite form, the polar surface is exposed when the dipole moment of the bulk unit cell is parallel to the surface normal [16]. In this case, the surface could either

be Zn-terminated or O-terminated.

Point defect	Type	Transition energy	Ease of formation
Oxygen vacancy	Donor	Deep/Shallow	Easy
Zinc intersticial	Donor	Shallow	Easy
Zinc antisite	Donor	Shallow	Medium
Zinc vacancy	Acceptor	Deep/Shallow	Medium
Oxygen antisite	Acceptor	Deep	Hard
Oxygen interstitial	Acceptor	Deep	Medium

Table 1.2: A brief summary of native point defects in ZnO [13]

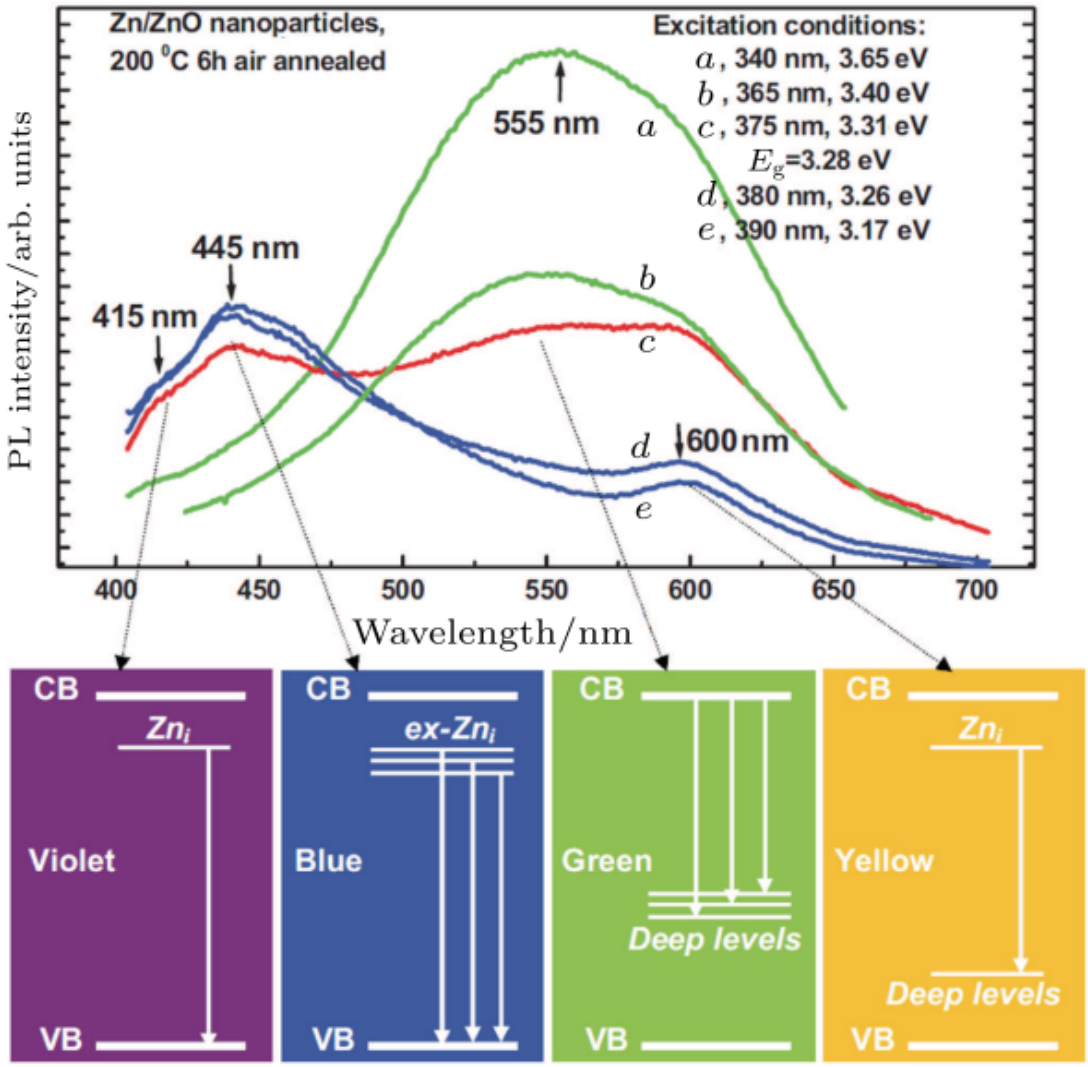

Figure 1.5: Excitation dependent photoluminescence spectra of air annealed nanoparticles along with proposed explanations of emission mechanisms [13]

Growth

ZnO particle sizes can be grinded from tens of microns to a few hundred nanometers in a planetary ball mill [17]. These ZnO nanoparticles have useful properties, as they can be alkyl passivated by an appropriate milling media, resulting in more stable dispersions. Nanoparticles produced by dry milling only have a tendency to agglomerate as the particle sizes reduce at higher energy milling conditions. Stable colloidal dispersions of zinc oxide are in high demand for a variety of industrial applications. The material is used in products like cosmetics, dyes, pharmaceuticals, ceramics and micro-electronics. It is also incorporated in composites such as rubber latex based formulations to improve the strength and homogeneity of the product [18].

ZnO nanostructures can also be grown from a bottom up approach, into 1D structures called nanorods. Nanorod growth is accomplished via vapor growth processes [19], and can also be accomplished in solution. Cored nanorod heterostructures are produced by sidewall epitaxy, by deposition of dopants along with Zinc and Oxygen on existing nanorods [18]. Nanorods have also been grinded in a planetary ball mill to induce surface functionalizations [20].

Other than the solution based spin coating [21] and sol-gel methods [22], thin films of ZnO of good quality are grown using molecular beam epitaxy (MBE), or pulsed layer deposition (PLD) [18]. The growth temperatures are not that high for ZnO, which is favourable for application on flexible substrates. In MBE, the growth is carried out in a low pressure chamber with separate sources of atomic Zinc (pure Zn metal) and Oxygen (plasma or ozone) that are evaporated and directed onto a substrate. The substrate is heated so that the molecules have enough energy to move around and find the lowest energy state to occupy, resulting in a perfectly packed structure. In PLD, a focused laser is pulsed onto a target material in a vacuum chamber. This cause ablation of the material, releasing a plume of molecules, ions and/or atoms, which are deposited onto an adjacent substrate. The oxidation of Zn occurs during ablation in PLD, as opposed to via surface reactions in MBE. ZnO thin films can also be fabricated via sol-gel processes, followed by spin coating.

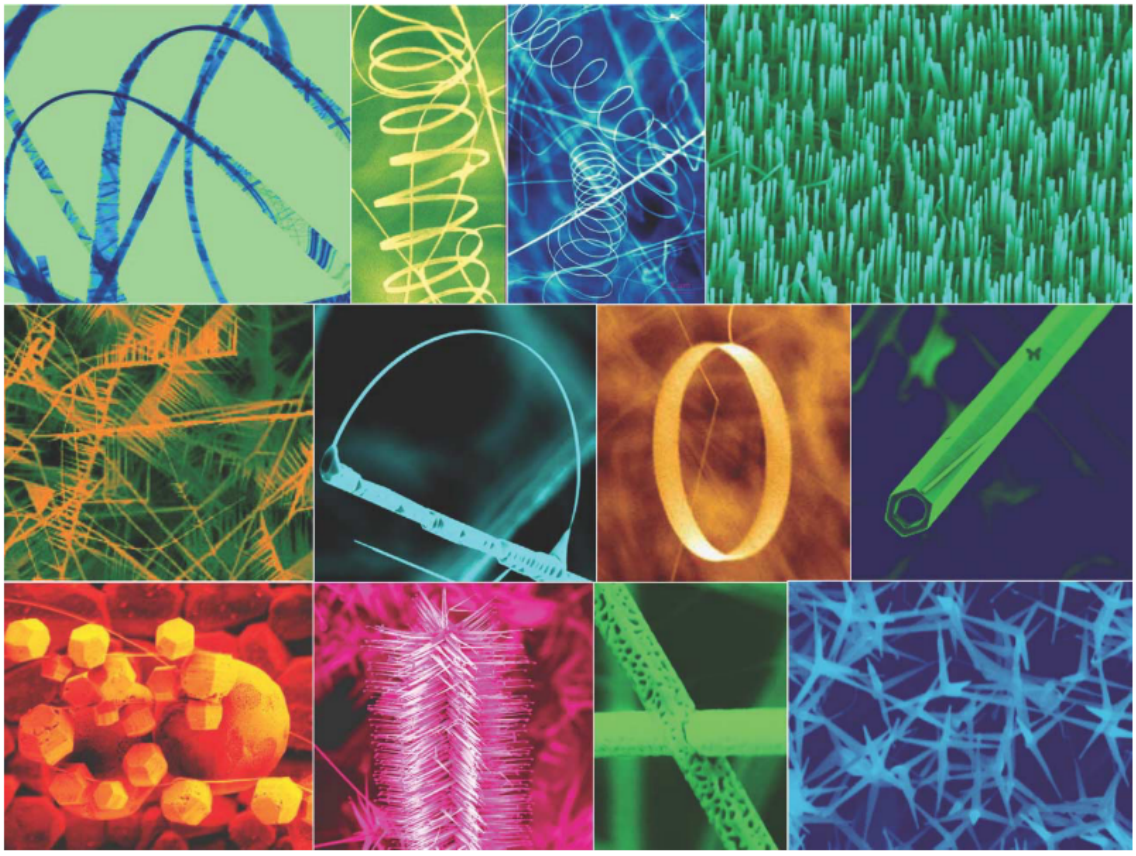

Figure 1.6: ZnO nanostructured formed by thermal evaporation under controlled conditions [6]

1.3 Properties of zinc oxide and their applications

ZnO nanostructures have found use in a variety of electronic applications including energy harvesting and conversion, and information processing applications such as transistors [23] and neuromorphic hardware. Well dispersed nanoparticles of ZnO can be used in inks to fabricate thin film electronic devices via inexpensive methods such as inkjet printing [24]. Such thin film electronic devices have use in applications such as solar cells [25][26], solid oxide fuel cells [27], thin film transistors [21], and light emitting diodes [28]. Zinc oxide nanoparticles have also been used in sunscreens and anti-microbial topical creams, and in as photocatalysts in conjunction with silver nanospheres [29].

In nanorod form, ZnO nanostructures have high surface area, making them suitable candidates for gas and chemical sensing applications. The ability to control their nucleation sites and grow them in an ordered pattern makes ZnO nanorods attractive for micro-lasers or memory array applications. Precise control over the heterostructures of cored nanorods is perfect for making arrays of devices such

as lasers or sensors that are fine tuned. The alignment of the constituent structures of the array is highly important in such device applications. Further, the growth process needs to be dependable and replicable in order to be commercially relevant, and zinc oxide nanostructures fulfil this criteria. In an alternate application, simple annealing of ZnO nanorods in hydrogen atmosphere has resulted in demonstrating resistive switching effects which makes the device a memristor [15].

As ZnO thin films require lower growth temperatures than Gallium Nitride (GaN), they are a suitable alternative as the material is less expensive and more abundant. The growth conditions of ZnO also allows the possibility of transparent junctions on cheap substrates such as glass, and flexible substrates such as plastic. With the relative abundance of Zinc compared to Indium, ZTO [30] is a cheaper alternative to ITO for electronic applications of transparent conductors, such as touchscreens.

1.3.1 Photoactivity

A semiconductor material can absorb a photon of higher energy than the band gap to create an electron hole pair. Thus when light containing the appropriate wavelengths is incident on a semiconductor, it results in an increase in conductance. This is considered to be a fundamental solid state process of photoconduction of semiconductors. The charge carrier pairs generated by the absorption of the photon would rapidly recombine in the absence of light, resulting in a sharp decay in conductance as soon as the light is removed. However, in the past decade or so it has been repeatedly observed that the response of n-type semiconductors, such as titanium and zinc oxides, show a conduction decay process that is very slow in comparison to the expected decay [31]. This effect is explained by the presence of atmospheric oxygen, which adsorbs on the surface in the form of a negatively charged ion in the dark, after absorbing a free electron from the n-type semiconductor. This creates a small depletion layer with low conductivity on the surface. When photons with energy higher than the fundamental absorption band of the semiconductor are incident on it, the holes produced near the surface are drawn to the adsorbed oxygen ions and discharge them. Thus, since these processes (other than the solid-state process) also contribute to the photoresponse, it is expected that the photoresponse will depend on the ambient atmospheric conditions surrounding the device, and indeed this is the case, as can be seen in figure 1.7. The authors measure the conductivity profile while toggling the irradiation of light and

measure the conductivity profile in various atmospheres. Without the presence of oxygen, there isn't much variation observed in the photoconductivity, suggesting that photoconductivity in ZnO films is not simply excitation of defect states, but the result of a more complex interaction with oxygen ions adsorbed on the surface.

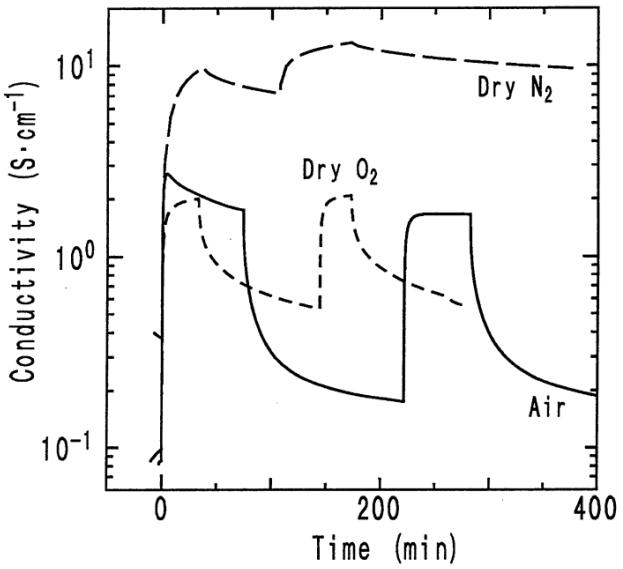

Figure 1.7: A ZnO thin film shows different conductivity profiles with varying atmosphere, suggesting the crucial role of adsorbates in determining conductivity of the films [31].

ZnO possesses a number of intrinsic and extrinsic radiative defect levels which emit light in a wide range within the visible region. Due to these radiative defects, ZnO exhibited various wavelengths covering the visible spectrum, such as violet, blue, green, yellow and orange–red colour emissions [19]. The energy band gap of zinc oxide corresponds to the energy of a photon in the ultraviolet range of spectrum, which indicates that this material is an excellent candidate for UV sensor devices. Moreover, the high exciton binding energy (60 meV) of ZnO ensures efficient excitonic emission at room temperature, and hence, luminescent properties are expected at room temperature with UV stimulation. Schottky type photodetectors have been fabricated on high quality ZnO epitaxial layers, which are grown on sapphire substrates by metalorganic chemical vapor deposition [32]. An example of the photoresponse to incident UV light on such a photodetector is showin in figure 1.8. The main problem for the application of ZnO as a material for electro-optic devices is ambipolar doping. This problem is frequently found for wide band-gap materials, where doping of one type (here n-type conductivity due to electrons in the

conduction band) is easily possible up to high densities, while the opposite type (in this case due to holes in the valence band) is hardly achievable.

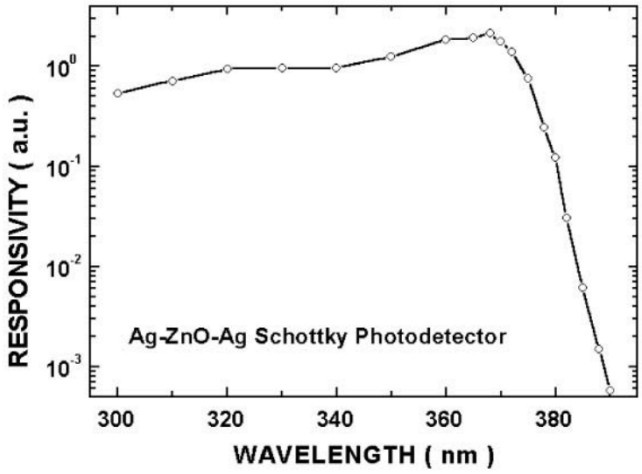

Figure 1.8: Spectral-photoresponse of a Ag-ZnO-Ag Schottky photodetector [32]

Besides its already high exciton binding energy, the ease of growth of ZnO nanostructures has led to improvements in various optoelectronic and photovoltaic applications. Researchers have demonstrated catalyst free selective ZnO growth on microstructured substrates made of other optoelectronic materials such as GaN [33], as can be seen in figure 1.9. ZnO nanoparticles have also been used as interlayer materials in organic solar cells, effectively replacing PEDOT:PSS to efficiently collect electrons and block holes in these bulk heterojunction solar cells [26].

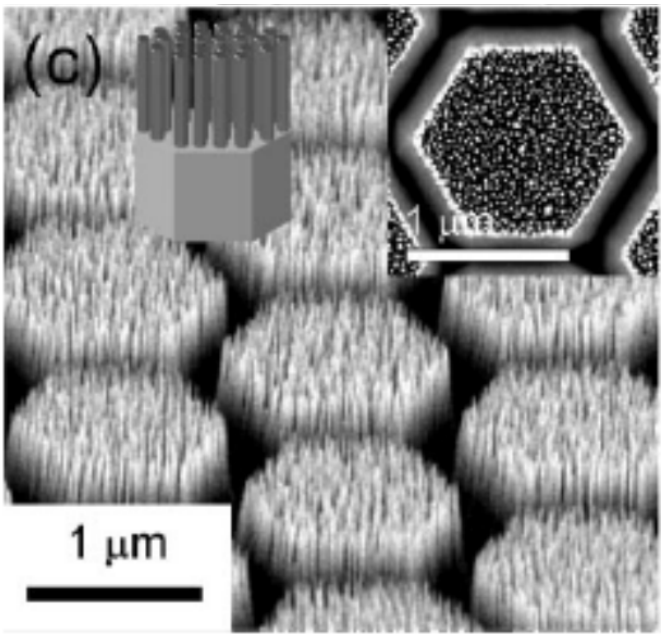

Figure 1.9: ZnO nanorods selectively grown on GaN microrods for photonic applications [33]

1.3.2 Memristance

Memory is persistent information that is accessible when required. It is an essential component of today's (Von-Neumann) computing architectures, where devices for computation and memory are separate. Even on the same die within a microprocessor, we have separate regions for short term memory (L1/L2 caches) and information processing (the arithmetic logic unit and/or look up tables). In practice, we can observe majorly two types of memory - fast and volatile (used in caches, RAM, etc), or slower and non-volatile (used for long term storage, like across reboots and disconnections of power). An example of the first type is SRAM/DRAM, while magnetic disk drives are an example of the second. Flash memory is also considered as permanent storage since it is non-volatile, and it is fast at the same time. However, it has its own set of problems such as needing error-correcting algorithms in the solid state drive controllers, because of device degradation after limited erasure cycles [34].

While some authors propose more exotic device implementations such as skyrmionic devices [35], practical nanoscale memory has to hold the promise to be integrated using current technologies, such as in the case of magnetic tunneling junctions. As current memory devices are based on electrical properties such as charge/capacitance (and measured by voltage/current), the nanoscale versions will also have similar properties. Three fundamental electronic devices are well established - the resistor,

capacitor and inductor. In 1971, Leon Chua proposed the fourth fundamental electronic device, aptly named the memristor [36]. This is a device which demonstrates a change in resistivity depending on the integral of the charge passing through it. Thus, in essence, the current state (encoded in the resistance) of such a device would be a function of its history - a phenomenon also known as resistive switching. Any device that behaves so via any mechanism can be called a memristor.

Memristance in a device can be bipolar (symmetric behaviour) or unipolar (asymmetric behaviour), depending on the underlying mechanism [37]. A very low 'READ' voltage pulse is used to probe the state of the device, with the aim that the current will be low enough to leave the resistance undisturbed. A slightly higher magnitude voltage is applied (sometimes in a series of pulses) to change the resistance of the memristor by an appreciable amount, called the 'WRITE' pulse. Until then, if there is no appreciable charge owing through the device, its resistance will not change, and thus it retains its state: non-volatile memory. Memristive devices often have a threshold voltage called the 'RESET' voltage pulse, which is applied (in opposite polarity, for long enough duration) to set the device to a default standard state [38]. In some devices, the underlying mechanism allows the change in resistance to be reliably continuous, such that any intermediate state can be reproducibly reached by the application of the same voltage pulses from the same state (for example, after 'RESET'). These are called multi-level memory devices, and their analog behaviour can be used to better represent biological synapses in hardware, in a field called neuromorphic computing [37]. They behave as both memory and computational units, allowing a non-Von Neumann computing architecture. However, in most devices, the switching behaviour is transient and non-ergodic, so we only consider the two extreme states of high and low resistance. The ratio of the resistances at these two states is called the ON/OFF ratio. Higher ON/OFF ratios are preferred as they are more easily distinguishable. Further, we would like the device to be able to switch between its states as fast as possible, and retain its state until manipulated, for as long as possible.

As a single multilevel resistance device has at least two states of resistance, it is sufficient to store a single bit of information. Compared to the multiple (2-4) transistors and resistors required to form a flip-flop, the use of memristors offers the same multiple of overall size reduction given similar feature sizes for the devices. Further, there is also a decrease in the number of connections required as the memristor is a two-terminal device. Since interconnects occupy the majority of the space on a chip,

a processor composed of memristors would be amenable to huge improvements in space and power efficiencies. Memristor devices can often have multiple memory levels beyond binary states, allowing for further innovation in computational device architecture. They can be used to construct the alternate paradigm of non-Von-Neumann architectures, exemplified in the field of neuromorphic computing [3]. Neuromorphic computing aims to approximate the computational functions in the human brain such as the phenomenon of activation potentials. The amount of information that a chip composed of multilevel memory devices can store/process scales exponentially with the number of states. In this architecture, the same device can be used for both information processing, as well as storage.

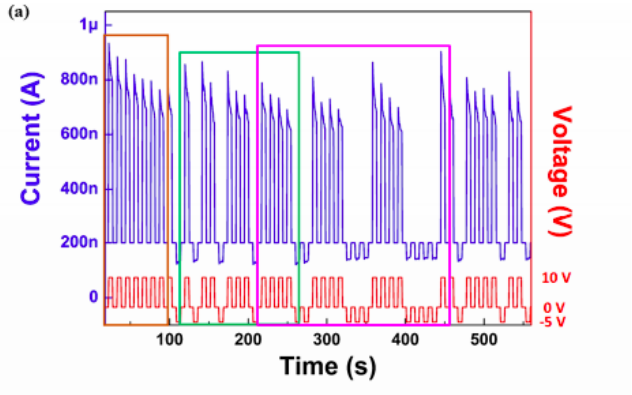

Figure 1.10: Current-voltage response over time of a ZnO-based memristor device fabricated with hydrogen annealing treatment [15]

The resurgence and proliferation of neural networks makes memristive devices particularly attractive for developing novel computational technology. There is a direct parallel between the multiple states possible in a memristor and the weights of a neural network. Memristors with many states are better understood as analog devices, as their conductance varies continuously. Crossbar arrays of memristor devices have been fabricated to perform hardware level machine learning tasks such as pattern recognition [37]. The memristors in these works mostly consist of a gradient of conductive ions in some matrix material, such as Ag ions in Si, in [3]. The distribution of ions along the gradient characterises the conductivity of the memristor. As charge flows through this memristor, it causes a change in the distribution of the gradient via diffusion of the ions, which in turn changes the conductivity, as depicted in figure 1.11. This way the device resistance is affected by its history, and represents the 'states' of the device.

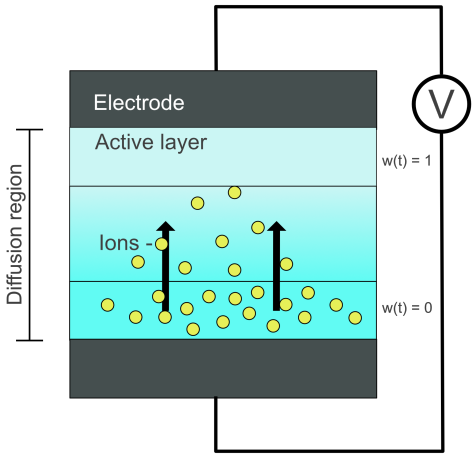

Figure 1.11: A schematic diagram of a diffusion controlled memristor device

Multiple devices of this structure can be fabricated in the form of a crossbar array, as depicted in figure 1.12. This is an efficient multiplexed planar architecture as $2n$ electrodes can read from and write to, n^2 individual memristor devices. Moreover, it is very feasible to construct with current fabrication technologies such as electron-beam lithography. Using appropriate representations, matrix operations can be performed in parallel on a hardware level. In [37] the authors fabricate a 32x32 memristor network array on a chip that interfaces with an FPGA, and use it to perform feature extraction from images.

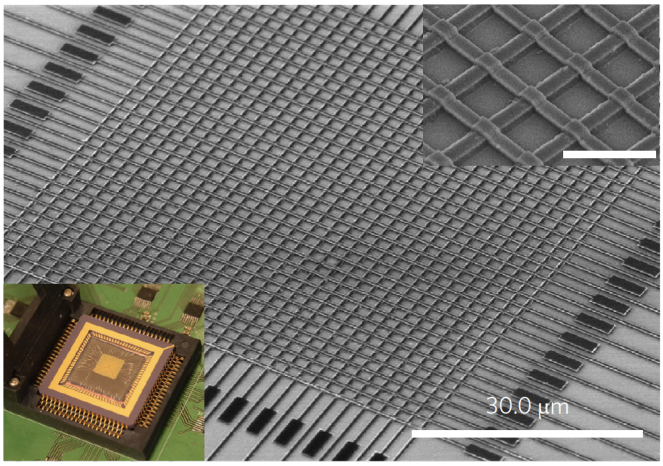

Figure 1.12: Scanning electron micrograph image of a memristor array, with an inset of a magnified SEM image of the crossbar [37]

1.3.3 Semiconductor junctions

The material under study is a semiconductor, and since silver electrodes are used for the measurement contacts, it is appropriate to idealize the devices to a metal semiconductor junction. Depending on the band structure and work function of the semiconductor and metal respectively, the I-V characteristics can be linear or rectifying. If the device displays a linear I-V characteristic, it is called an Ohmic contact or device, while a rectifying characteristic means that the junction is a Schottky barrier, making the device a diode. The following is background material summarized from a textbook on solid state electronics [39].

Rectifying contact

When they are not in contact, the band diagrams of a metal and n-type semiconductor will be similar to that shown in figure 1.13. E_o is the energy required for an electron to escape into vacuum from the material, termed the vacuum energy level. It is a common reference energy level to use when comparing the electronic properties of dissimilar materials. E_{FM} and E_{FS} are the Fermi levels of the metal and semiconductor, respectively. The Fermi level of a material is the energy level at which there is a 50% probability of an electron occupying that state. Another way of understanding it is as the average of the energy levels of the electrons in the material. Thus, the difference between the vacuum energy level and the Fermi level of a material is labelled the work function of the material. Since the Fermi level of a given metal doesn't vary, the work function of a metal (Φ_M) is a fundamental property. However, the Fermi level of a semiconductor changes from instance to instance, depending on the carrier and dopant concentrations. Consequentially the work function of a semiconductor (Φ_S) also changes, and systematic predictions cannot be made. Thus for semiconductors it is more convenient to characterize their electron affinity(χ), which is the difference between the vacuum level and conduction band energy levels of the material.

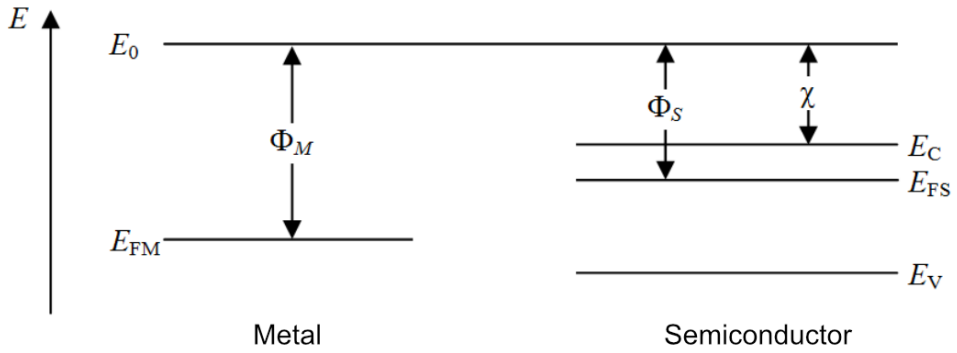

Figure 1.13: Energy band diagrams of a metal and semiconductor (n-type) in isolation from each other

When these two isolated materials are brought in contact, they form a junction. At first the carriers diffuse according to the balance of energy levels. In this case, the electrons from the semiconductor diffuse into the metal to occupy the lower energy states that are available. The reduction of the number of electrons in the semiconductor reduces Φ_S. There is a negative charge from the excess electrons in the metal surface, and an equal positive charge from the vacancies left behind in the semiconductor. This creates an electric field in the opposing direction of the flow. The strength of this field increases as the diffusion of carriers continues, and soon it is strong enough to prevent further diffusion. This leads to one overall Fermi level for the materials and their junction at thermal equilibrium, when $E_{FM} = E_{FS}$. Figure 1.14 shows the idealized situation at thermal equilibrium when a metal and n-type semiconductor are brought into perfect contact with each other. The band bending represents the loss of negative charge from the semiconductor. The amount of bending is a product of the charge of the carriers (q) and the built in potential (V_{bi}) that results from the number of those carriers leaving the semiconductor.

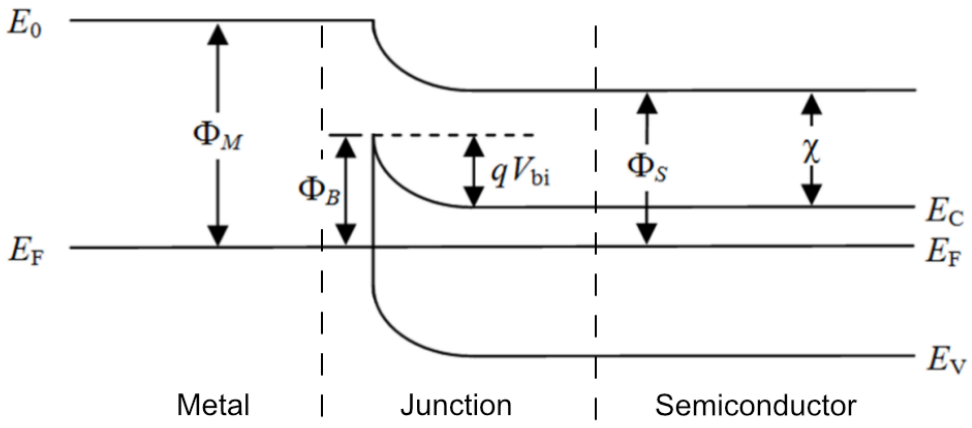

Figure 1.14: Energy band diagrams of a metal-semiconductor (n-type) contact junction

Since the work function of the metal(Φ_M) and electron affinity of the semiconductor(χ) are fundamental properties, they remain constant. From the metal side, there is a barrier of height Φ_B which is numerically equal to $\Phi_M - \chi$. Since it is dependant on constants, this barrier height is also a constant and will not change with applied voltage. This means the same number of electrons will cross the barrier in that direction, regardless of the applied bias. This amount is called the reverse saturation current(I_o). From the semiconductor side, the barrier is defined by the amount of band bending. Since that is dependent on the built-in bias, and is affected by applied voltage. Thus, when the negative terminal of the applied voltage is on the side of the n-type semiconductor (forward bias), the barrier will decrease with increasing voltage.

The I-V characteristics in the ideal case is shown in figure 1.15. However, in reality, there is no perfect contact between the materials. At the surface of the semiconductor, some covalent bonds may be unsatisfied, leading to interface states. There may also be additional surface states caused by surface roughness. Even on the metal side, surface roughness may affect the work function slightly, as predicted for Ag [40]. These defect states can trap charge and alter the value of Φ_B and I_o. In the case of nanoparticle films, as fabricated for study in this report, there are an even greater number of surfaces and other variables, such as presence of trace amounts of solvent, that can lead to deviation from ideal behaviour. In particular, the inter-particle junctions are likely to contribute to an overall series resistance which would greatly dampen the exponential increase in current as shown in figure 1.15.

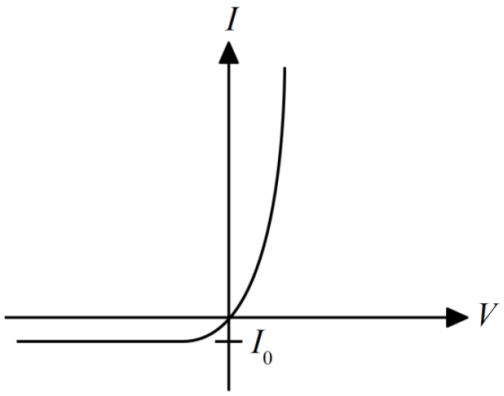

Figure 1.15: Current-voltage characteristics of an ideal Schottky barrier diode

Ohmic contact

An ohmic contact is a junction that behaves almost like a resistor. The voltage drop across the metal-semiconductor junction is very close to zero. In the case of an n-type semiconductor, this happens when the work function of the semiconductor is greater than that of the metal, and the elecron affinity of the semiconductor is very close in value to the work function of the metal. In this case, there is no barrier when the applied bias causes electrons to flow from the metal into the semiconductor, and little to no barrier when bias is applied in the opposite direction. The barrier in this direction is also reduced by heave doping of the semiconductor such that its Fermi level is raised close to its conduction band edge. When such suitable materials cannot be selected, an ohmic contact is achieved by extreme doping of the semiconductor, which causes a very large, and also very thin barrier. Given that the barrier is sufficiently thin (10nm), the carriers can tunnel through it to achieve conduction.

Metal-Semiconductor-Metal junctions

A metal-semiconductor-metal (MSM) junction can be considered as two metal-semiconductor junctions placed back to back. In the absence of applied bias, the energy band diagram of the junction will look like figure 1.16 in an ideal case. When a bias is applied, the energy levels will be as in figure 1.17, for the case where the positive terminal is connected to the left side and the negative terminal is connected to the metal on the right side. Thus the left junction will be forward biased while the right junction is reverse biased, and vice verse when the applied voltage is reversed. This results in a current voltage

curve as depicted in figure 1.18.

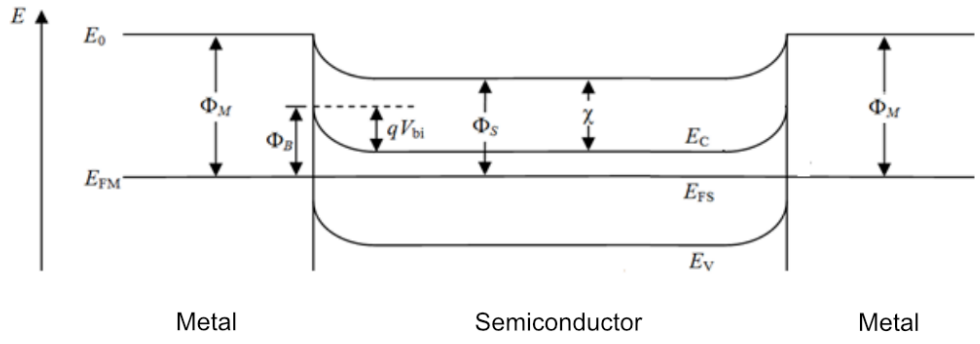

Figure 1.16: Band diagram of a metal-semiconductor-metal junction at thermal equilibrium

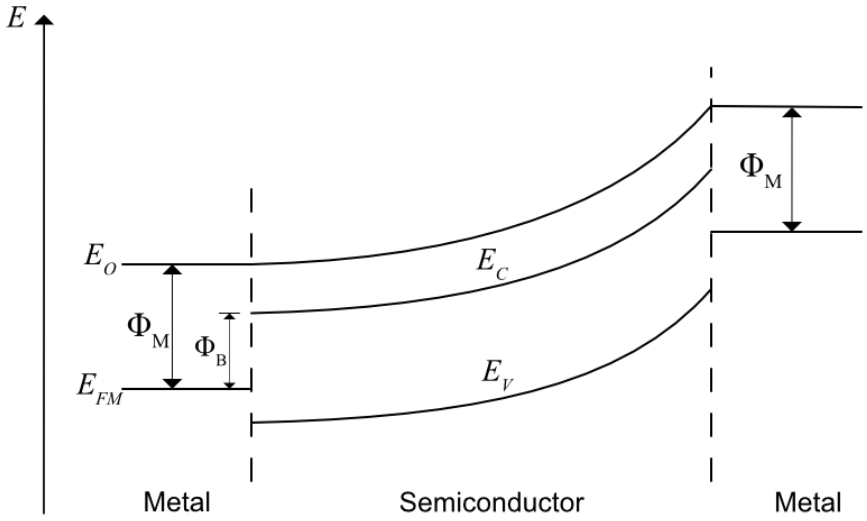

Figure 1.17: Band diagram of a metal-semiconductor-metal junction under applied bias

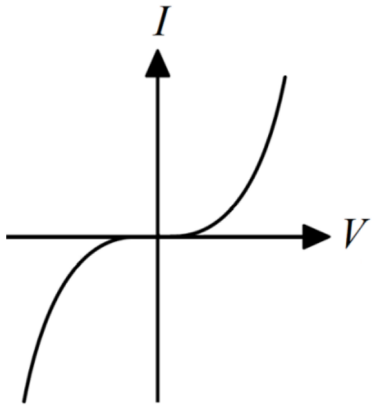

Figure 1.18: Current-voltage characteristic of back to back Schottky diodes

1.4 Report outline

In this work, we study the electronic properties of zinc oxide nanoparticles fabricated by planetary ball milling, by constructing two terminal thin-film devices and measuring their current-voltage response characteristics under various conditions. This chapter elucidated the motivation and background for the rest of the report, by introducing some challenges in the semiconductor industry, the need for novel material applications, and the properties and potential applications that make ZnO an interesting material to study. The second chapter focuses on the experimental methods used in this study. We start with the fabrication method, which is planetary ball milling, and after describing the process and its parameters, move on to the characterization techniques used to collect data about the fabricated material and devices. This data is analysed in the next chapter (Chapter 3), which provides the main results of the study undertaken. Here we discuss the observable effects, which we obtain by having controlled various fabrication parameters. The effect of light, thermal annealing, and grinding speed on the conducitivity of the ZnO thin films was studied. The effect of mixing ITO with ZnO during grinding was also compared, in terms of electrical properties. Finally, Chapter 4 concludes with some suggestions for future work to perpetuate the direction of inquiry of this report. Some of the results of this work have been published in an article about multifunctional thin-films [41].

Chapter 2

Experimental Setup and Procedure

2.1 Nanoparticle Synthesis

2.1.1 Planetary Ball Mill

Nanogrinding is an efficient top down mechano-chemical approach to fabricating nanomaterials. Obtaining smaller particle sizes is one of the most important unit operations in many industries because of the advantages obtained by such a change in material. Smaller particle sizes result in larger net surface area for any given mass of material. In cases where the surface area is important owing to its chemistry, this gain is highly desirable. Usually starting from powder form, a material is subject to multiple high energy impacts that break down the particles to smaller and smaller sizes. Due to the high energies at the points of impact, chemical changes may also take place in the material as bonds are broken and re-formed. Therefore, high energy milling is referred to as a mechno-chemical synthesis technique. High energy mechanical milling has been used to fabricate a variety of nanomaterials such as alloys, nanocrystalline powders, nanocomposite powders, etc [42].

One of the most used types of milling devices in the laboratory is the planetary ball mill. Compared to mixer mills or stirred media mills, planetary ball mills are preferable due to the moderate cost of the device and its operation, simple set up and material processing steps, and good cleanability [4]. They are also preferred in the laboratory due to good reproducability, comparatively short processing times, and safe handling. The planetary ball mill (PBM) is highly efficient for the purposes of ultra-fine grinding

and mixing of materials. It has been used to create interesting materials for various applications in academia as well as industry. The advantages of this route include reduction in the amount of reagents, reduction in reaction times, as well as production of higher yields, resulting in an overall more efficient use of resources like materials and energy [43].

Planetary ball milling is a technique that has been known for more than a hundred years. The device normally has 2 or 4 pots for grinding materials. The pots rest on a planetary disk. The planetary disk rotates around a common central axis while the pots, or jars simulataneously rotate around their own axes. The jars are filled with the material to be grinded, and milling balls made of a very hard and comparatively inert material. The high rotation energies of both types of movement works together to produce very high impact energies of milling balls in the jars. These high energies lead to effective grinding performance as the particles are crushed between the milling balls by the frictional and/or impact forces of the collisions.

The rotational speeds and directions of the pots and the planetary disk together combine to a positive or negative ratio that contributes to the behaviour of the milling balls. Further, a charge on the powder may also develop, that affects the motion of the balls inside. The pattern of motion of the milling balls affects the number of collisions, the ball velocity, and the energy dissipation [42]. The movement of the balls inside the jars is complex and depends on the parameters selected for operation. The pattern of their movement ranges from cascading to cataracting to rolling, with increasing filling ratio, and increasing revolution speed [44]. As can be seen in Figure 2.1, in the cascading regime, the milling balls are transported along the walls of the jar to the top of the bulk, from where they fall upon each other towards the base. Opposed to this is the rolling regime, when the forces acting on the milling balls inside the jar are so large that they are stuck to the sides as it rotates, with almost no relative velocity to each other. In between the cascading and rolling regimes we have the catacracting regime, where the balls are carried up by the walls and then detach with high velocity to impact the rest of the bulk or the opposite walls.

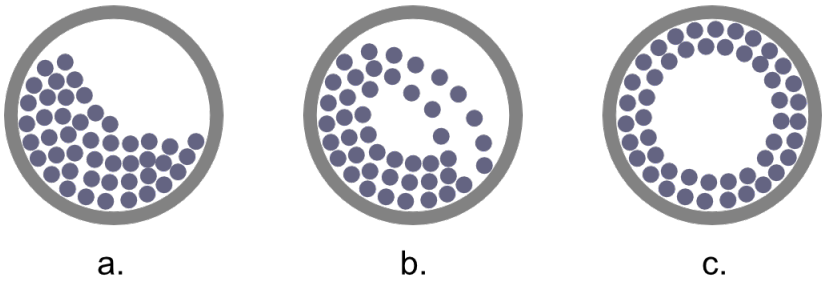

Figure 2.1: Milling bead movement regimes - a. Cascading, b. Cataracting, and c. Rolling

Having such a complex nature, it is important to consider the most relevant parameters of the process. These are [5]-

- Revolution and rotation speeds, at a constant speed ratio
- Duration of the milling process
- Filling ratio of the milling balls to a given jar volume
- Filling ratio of the milling balls to the powder materials

These parameters are not independent of each other, as the exact behaviour inside the PBM is highly unpredictable and not easily observed or described. However, these parameters can be empirically optimised to obtain the best yield and refinement of particles via control over the kinetics. Numerical studies have also been carried out [44] to study the effects of rotation to revolution speed ratios and rotational directions. It was concluded that the counter direction of rotation to revolution results in higher impact energies in the ball mill, compared to the normal direction where the jar rotates in the same direction as the revolution. There is an increase in specific impact energy with the increase in rotation to revolution speed ratio, up until the point of critical speed when the balls start the rolling motion. The rolling motion is undesired and the cataracting regime is preferred to obtain the highest efficiency from the energy put into the operation of the PBM.

Another important parameter is the presence or absence of a solvent while grinding. This is termed wet or dry grinding respectively. In dry grinding, powder of one or more materials is placed in the jar along with the milling beads. The energy from the impacts is transferred directly to the solid state

material and results in particle breakdown. If more than one material is used, there may also be reactions between the materials such as alloying. Grinding in the presence of a solvent can have advantages such as better heat dissipation, better homogeneity, easier extraction of the grinded material, and capping of grinded particles to mitigate agglomeration. Organic synthesis reactions have also been carried out in a ball mill [5]. However, this can also be a disadvantage when the reactions are unpredictable and lead to undesirable functionalization of the particles. The presence and composition of such coatings can be verified by purifying and characterizing the grinded materials with technicques such as Energy-dispersive X-ray spectroscopy and Raman spectroscopy.

For this project, we control the rotation speed of the milling procedure while trying to keep other parameters constant for a given material/batch. The milling procedure was performed in a Fritch Pulverisette 7 Micro Mill (shown in figure 2.2). This piece of machinery has slots for two jars, one of which was used for milling and the other was filled with the appropriate counterweight. The jars are made of silicon nitride with a capacity of $80mL$. The milling balls used for grinding were Zirconia beads of $2mm$ diameter. Generally, a ball to powder ratio of 50:1 was used. With all the milling beads weighing in at 100g, this corresponds to a powder weight of 2g being used per milling trial.

Figure 2.2: Fritch Pulverisette 7 Micro Mill

A duration of 10 minutes was chosen for milling. This is a value that can be modified in future studies as it was decided to use a constant duration for all the trials. This way, the effect of grinding speed can be compared across trials. The PBM machine was configured to perform the grinding in two runs of 5 minutes each with a rest time in between. The rest time is necessary because heat builds up very quickly from the frictional forces inside the jar. It is also useful to perform routine checks on the jar. From previous experience with the pressure build-up inside the jars, the following practice was implemented

while performing the grinding procedure - the seals of the jars were examined during the rest time, as well as after the trial, to detect any leakage that might occur. In the case of trials at higher speeds, the rest time was increased.

Trial	Speed (rpm)	Duration (mins)	Rest-time (mins)	Medium
200a	200	10	5	EG
400a	400	10	5	EG
600a	600	10	10	EG
800a	800	10	10	EG
1000a	1000	10	15	EG
ZnO-IPA-1	200	10	5	IPA
ZnO-ITO-IPA-1	200	10	5	IPA

Table 2.1: Parameters of the grinding trials

2.1.2 Materials

The primary material used in this project was Zinc Oxide (ZnO), which was grinded at various parameters discussed below. The powder used was 99% purity, obtained from VWR Chemicals. ZnO has attracted considerable interest in academia in the past 6-7 decades or so thanks to the many applications, knowledge of its properties and growth and processing steps. Powders of ZnO have been reduced to nanoparticle sizes via ball milling in various studies [17][24] and the result can be seen in figure 2.3. Over the course of milling for longer durations, they observed that certain wavelengths of the photoluminescense spectra between 350nm and 600nm diminished, while others increased. Moreover, the initial bands were sharp while the new bands were broader. This is due to the distribution of defects among the particles changing because of being subjected to the milling process. The authors of [17] also report the lattice relaxation along the polar surface of the structure. They attribute this to the effect of strain caused by the loss of oxygen ions, which they deduced from the photoluminescense spectra.

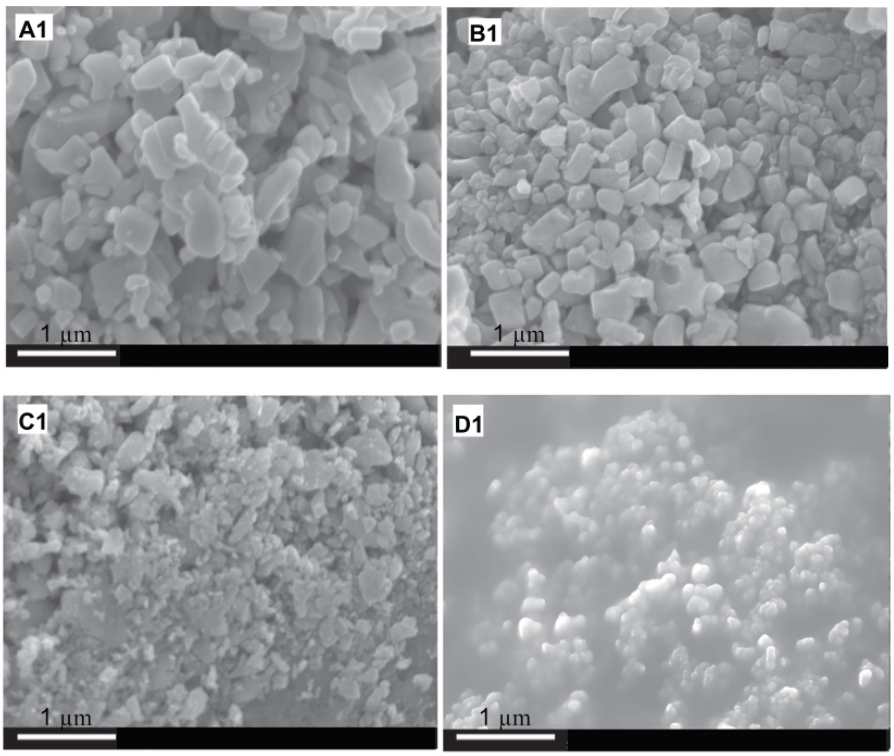

Figure 2.3: Scanning electron microscope images of ZnO milled for increasing durations [17]

It is possible to grow epitaxial layers, quantum wells, nanorods and quantum dots of ZnO relatively easily and reliably [6]. In the form of these nanostructures with special electronic and material properties, ZnO can be used for [9][12]-

- Optoelectronics - light emitting diodes or photosensors in the blue and UV region
- Electronics - as a semiconducting circuit material for band engineering
- Electronics - as a piezoelectric material for small scale electromechanical sensing
- Electronics - as an active material for gas sensing
- Electronics - as a highly conducting transparent material, when doped with Al, Ga, or similar elements
- Spintronics - as a ferromagnetic material, when doped with Co, Mn, Fe, or similar elements

The use of zinc oxide nanostructures for their memristive properties has also been demonstrated [45]. These devices exhibited history dependent voltage response behaviours as shown in figure 1.10. In

one study [46], the deposited dispersion was annealed at temperatures as high as 500℃, which is still only about 34% of the absolute melting temperature of ZnO, which is 1975℃. This study confirmed that organic species were removed and a wurtzite hexagonal polycrystalline structure was formed by annealing the material, from X-Ray Diffraction and Raman spectra. In [15] a single nanorod of ZnO is isolated and connected to gold electrodes, after which it is annealed in hydrogen. It is reported that the differential resistance observed arises from trapped electrons in an amorphous ZnO interfacial layer formed by the annealing process. In the low voltage region the conduction is initially Ohmic, and at higher voltages the current scales proportional to the square of the voltage, which is consistent with trap-controlled space charge limited conduction. This occurs because at higher energies, trap states become energetically accessible and the injection of charge carriers from the contact leads to the formation of a space charge layer. Thus as the rate of trapping overtakes the rate of detrapping, there is a downward shift in the slope of conduction.

It is evident that many of the desirable properties of zinc oxide arise because of defect states, and these defects can by tuned by various fabrication and processing steps. Further, in the case of nanoscale materials, there is a much higher surface to volume ratio, and therefore also a higher defect to volume ratio. This means that we can likely enhance the desirable properties of zinc oxide by processing it to nanoscale dimensions. Using highly controlled growth parameters it is possible to tailor the material (for example controlling the emission spectra via the width of fabricated nanorods for lasing applications). For this it is important to know the variations in the behaviour of the material before it can be tuned. For this report we are not interested in optical properties and focus on the electrical properties of ZnO nanoparticles.

Tin-doped indium oxide, or indium-tin-oxide (ITO) was also used in one of the trials. It is a well known transparent conducting oxide that has found use in electronic applications such as displays and solar cells. To achieve the extremely high levels of conductance along with 80% optical transmittance in the visible region, thin films of ITO have been annealed at 250℃ or higher [47]. Nanoparticles of ITO in a narrow size range have been produced by colloidal chemistry [48], however, here we reduce particle size by milling as well. ITO powder was used along with ZnO in a grinding trial to observe if mixing the materials during ball milling produced changes in the electrical properties of the films fabricated later.

2.1.3 Extraction

After grinding, the jars were allowed to cool down so that the pressure inside normalized. Then the slurry was extracted from the jars with the help of a syringe. The equipment used for extraction consists of a fitting specially made for the jars that causes the grinded material to pass through two stainless stell meshes and is sealed airtight with rubber O-rings. As all the material cannot be extracted in the first draw of the syringe, the extracted material in the jar was replaced with an equivalent amount of solvent and the next extraction was performed. These draws from the syringes were stored in separate vials of decreasing solid particle density, and were labelled alphabetically according to their order. The extracted suspension was stored in vials for several reasons:

- The vials can be easily stored and labelled.
- Since the vials are transparent, there is an immediate visual representation of the amount of material remaining.
- The vials have threaded caps that were additionally sealed with parafilm to prevent contamination and leakage. This way there is less likelihood of accidental spills or evaporation of the solvent over time.
- The nanoparticles tended to settle at the bottom after a while, and these smaller containers can be sonicated more easily, without the need for transferring to another container, resulting in wastage of material along the sides.
- The ground material needed to be accessed frequently from its container for fabricating films. The vials are very convenient for extraction via a micropipette for this purpose.

2.2 Device Fabrication

Prior to fabricating the thin films for further study, the vial to be used was vigorously shaken for a minute and then sonicated in an ultrasonicator (VWR ultrasonic cleaner with digital timer) with a power level of 5 for one minute. This step was performed to undo any light agglomeration that might occur due to Van der Waals forces [49].

Following the dispersion step, the thin films of ZnO were fabricated via drop casting. Drops of a uniform size (3μL) of the ZnO particle-containing solvent were extracted with a micropipette and deposited on a glass slide substrate. Four films were deposited on each glass slide. This ensured that they undergo similar conditions for drying, as much as possible. It is also good to have multiple films on the same substrate to ensure repeatability, and in case of variance, it is more apt to approximate from as much independent data as possible. The films were then dried in a mechanical oven, Lindberg/Blue MO1440A-1, also at various temperatures. For the exact details please refer to table 2.1. A batch of films after drying is depicted in figure 2.4. After drying, contacts were deposited onto the film using silver paint and the film was placed in the oven once again for additional time, usually 30 minutes, to evaporate the solvent of the silver painted electrodes.

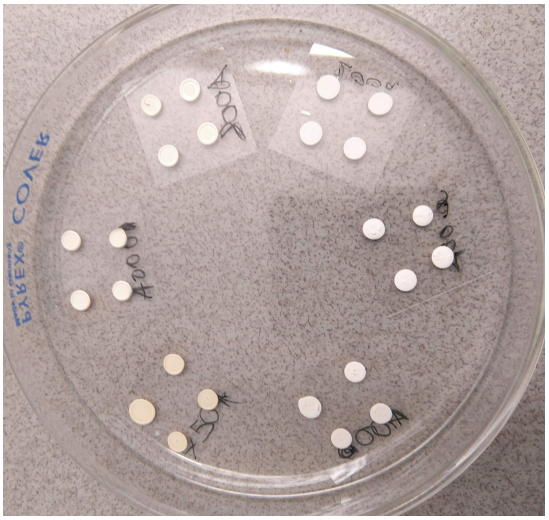

Figure 2.4: Films of various trials after annealing

2.3 Electrical Characterization

Once the two-termical thin films devices were fabricated, their electrical properties were charaterized. This was done using a Keithley 4200 semiconductor Characterization system in conjunction with a Janis probe station. The probe station along with the microscope connected to a digital display allowed precise placement of electrodes. A schematic of the setup is shown in figure 2.5. The measurement itself was configured and recorded via an integrated Keithley Source-Measure Unit. The 4200-SMU can measure current in the range of pico-amperes, with the resolution of a femto-ampere and accuracy of 0.1% or less.

Voltage was applied across the two terminals of the device and the corresponding output was measured. Starting from lower voltages, a sweep of -5V to +5V was performed on the films with a step size of 0.05V. The voltage sweep was carried out repeatedly to get an idea of the electrical behaviour of the ZnO thin film devices. Consecutive measurements on the same film showed slightly varying behaviour, so multiple measurements were recorded and exported to spreadsheets. Python code was written to extract the data, calculate averages when necessary, and plot the measured values. Even if they are made from the same vial, each of the films are independent from each other for the purposes of electrically characterizing, once they were dropped and dried.

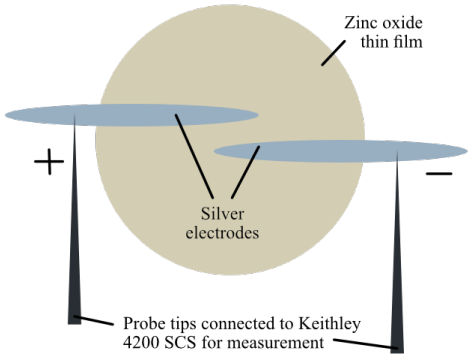

Figure 2.5: A schematic of the measurement setup. The two probes apply a programmed voltage sweep on the electrodes and the current response data is recorded using the Keithley 4200SCS.

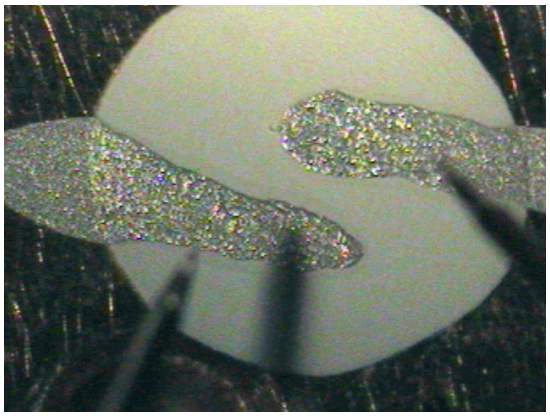

Figure 2.6: Closeup of a single film along with probes (the two shapes slightly out of focus) before they are lowered for measurement. Also visible are the contacts made of silver paste on the drop casted thin film made from nano-grinded zinc oxide.

2.4 Summary

Planetary ball milling is the nanofabrication technique used in this study. Particles of ZnO were grinded to reduce their size. The parameters of the grinding procedure were kept as uniform as possible across trials, while the grinding speed was varied across trials. In one case, ITO was also grinded along with the zinc oxide. The grinded material was extracted into different vials, which were first shaken and then sonicated before being used to fabricate the thin film devices. Drops of 3µL volume were cast onto glass substrates with a micro-pipette. In some cases, patterned gold electrodes were used. The films were then dried in the oven and after electrodes were painted onto them with conducting silver paint, the electrical properties of the films were measured in a Keithley 4200SCS.

Chapter 3

Results and Discussion

3.1 Optical Inspection

After deposition and drying, preliminary optical characterization was carried out. The films were inspected optically to discern any obvious defects in fabrication. Deformations can be caused if there are bubbles during depostion of the drop. Cracks can also be caused by the drying process. The fabrication for that batch was repeated if glaringly discernible defects were found. In the films used for electrical measurements, no such defect is to be found. The films were found to be fairly compact and uniform in most cases. The films made from the mixture of ZnO and ITO had a slight tinge of green in their appearance, most likely owing to the color of the ITO powder. As the films were not annealed at very high temperatures, the color of the films did not change noticably after the heating/drying process.

3.2 Electrical Characterization

Once the devices were fabricated and the electrodes were dried, they were allowed to rest at room temperature in a covered petri-dish. To measure the electrical properties of the nanoparticle films, the glass slides were transferred to the probe station carefully, using a vacuum suction tip to avoid damaging the films. There were a set of four films of the same grinding batch per slide, with markings on the corners of the glass slide to identify them. Keeping track of each individual film is important

to accurately determine the change in properties being studied. The probe station has a microscope connected to a screen to manipulate the probes with precision. Once the film under observation was focused under the microscope, the probes were moved into position above the film and then gently lowered onto the electrodes. Both the probes were first placed on the same electrode to check proper conductivity of the contacts. Once the integrity of the painted silver electrodes was verified, the probes were put in position to measure the current-voltage characteristics of the thin film.

The films were first probed from -1V to +1V as a preliminary measurement, as shown for a film of unground material in Figure 3.1. After it was verified that the films weren't damaged by the current flowing through them, the range of voltage was increased. For most of the measurement data used in this report, the voltage was varied from -5V to +5V in steps of 0.25V and the Keithley was set to automatically set the compliance. In some cases the voltage range was lower, as is apparent from the figures.

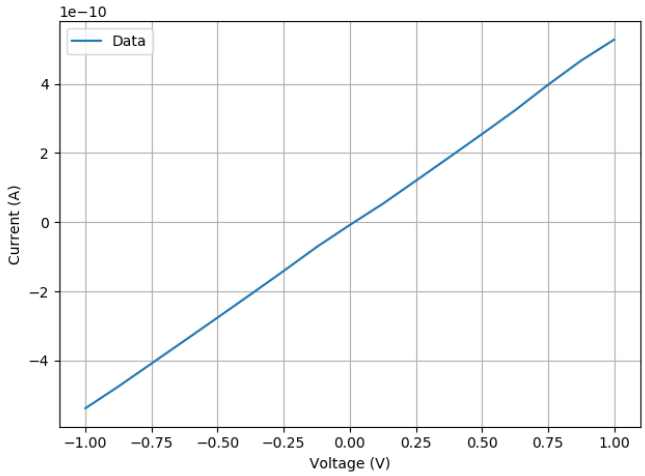

Figure 3.1: I-V characteristic of a film made from bulk powder

3.2.1 Effect of light

To verify the effect of light on the films, a variable brightness lamp was used to shine light onto the film inside the probe station during measurement. The brightness of the lamp was controlled with a dial. Measurements were taken with full brightness, then with the dial at half of the maximum brightness, and then finally with the lamp turned off. This measurement procedure was repeated for all the films in the batch being measured. For this batch, four films each of trials 200a, 400a, 600a, 800a, and 1000a were

fabricated on glass slides. The films were heated for 3 hours at 100℃ after which electrodes were painted on two of the films on each slide, and they were all left in the oven for 30 minutes at 80℃. Following this all the films were annealed at 200℃ for 2 hours, and then silver paint was applied on the remaining two films on each slide. Then they were heated for 15 minutes at 100℃ for the silver paint to dry.

Following this preparation the films were characterized with a voltage sweep of -2V to +2V at step sizes of 0.025V using the procedure described above. It can be seen that the conductivity of the nanoparticle films increases in the presence of light and is proportional to the intensity, as can be seen from the plot of a film fabricated from trial 400a, in figure 3.2.

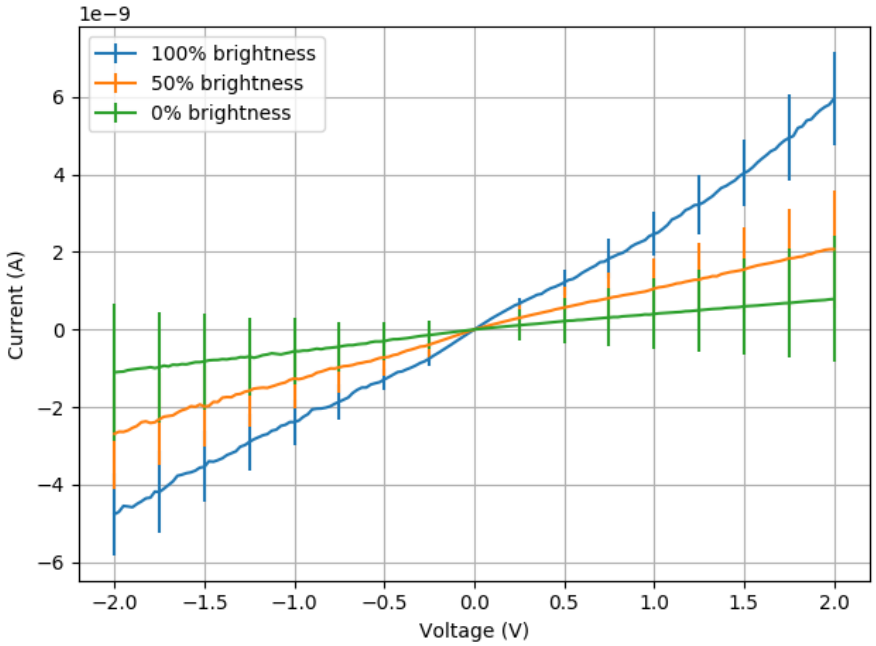

Figure 3.2: Varying brightness on consecutive measurements on the same film. Error bars indicate the range of values over which the average was taken.

3.2.2 Effect of annealing

To study the effect of heat on the films, we fabricate films, measure their I-V characteristics, anneal them further, and measure the I-V characteristics again. As there are many unpredictable variables, each run gives a slightly different I-V curve. Even on the same film, consecutive measurements at the same parameters will not be exactly the same. This may be due to the unpredictable nature of the current paths in the film, and factors such as surface roughness, etc. To isolate the effect of heat from

this variability, multiple consecutive measurements were taken at each annealing step and the average values of the current at every voltage level was used to construct an I-V curve to represent that step.

Four films of 3µL from the second vial of the trials were fabricated by drop casting and labelled individually. They were annealed at 100℃ for 3 hours, after which silver paint electrodes were applied and the films were left to dry at 80℃ for 30 minutes. The films were then measured with a voltage sweep of -5 to +5 V multiple times consecutively. After that annealing was performed for an additional 2 hours at 200℃ and 15 minutes at 100℃. One of the films from trial 400a was used to generate the plot shown below (figure 3.3). Since all the data for this plot are from the same film, there is no variability in electrode placement. It can be seen that the current response averaged over consecutive measurements increased with the additional annealing process. This trend is fairly consistent across the films of all the trials. The reduced resistivity due to additional annealing can be attributed to the facilitation of better bond formation between the particles in the film. Further experimentation can verify this hypothesis, and further characterization techniques such as x-ray diffraction analysis can be used to determine if the changes in the crystal structure/grain size due to annealing.

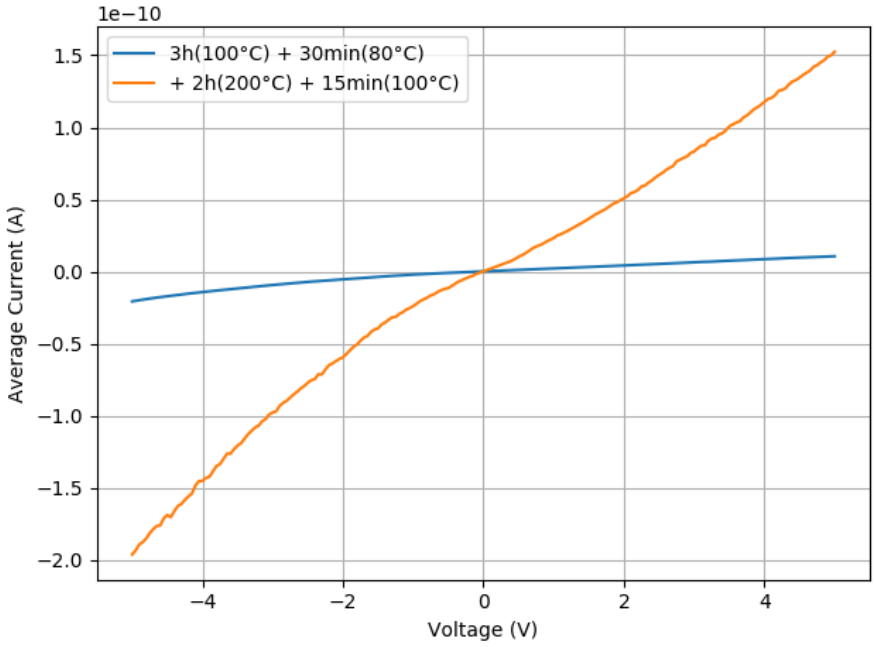

Figure 3.3: Average current response for a single film after extra annealing

3.2.3 Effect of grinding speed

There has been prior work done on the effect of grinding time on particle sizes of ZnO[17][49]. From this it is safe to hypothesize that nanoparticles produced from the different grinding trials will have different sizes, and this may affect the conductivity of the nanoparticle films. Since the active device dimensions and electrode spacing was not precisely controlled in this work, it would not be statistically relevant to compare single measurements of films across trials. However, with enough measurements we can approximate the effect of varying grinding speeds due to the central limit theorem. Without knowledge of the distribution of resistivity for individual films, a large enough number will tend towards a gaussian distribution. Thus taking the average for films prepared under the same conditions from each trial can be statistically relevant information.

Films of grinding trials 200a, 400a, 600a, 800a, and 1000a were used to fabricate films as described in the previous section. They were all measured in the absence of light. It can be seen from figure3.4 that in general, the conductivity of the films decreases with increasing milling speed. This can be expected due to the decreasing particle sizes. As the size of particles reduces across trials, assuming a uniform mass density, there will be more particles per given volume in the films made from trials with higher grinding speeds. Thus there will be more interparticle junctions that contribute to the overall resistance. However, this trend does not hold in every case for the data measured during this work. This can be explained because the movement of the milling balls may be entering the rolling regime beyond a critical speed. The precise value of the critical speed for this case is unclear. Further, the reduction in difference between the properties of films grinded at higher speeds can be expected as the milling enters the rolling regime, thus providing minimal increase in specific energy on increasing speeds.

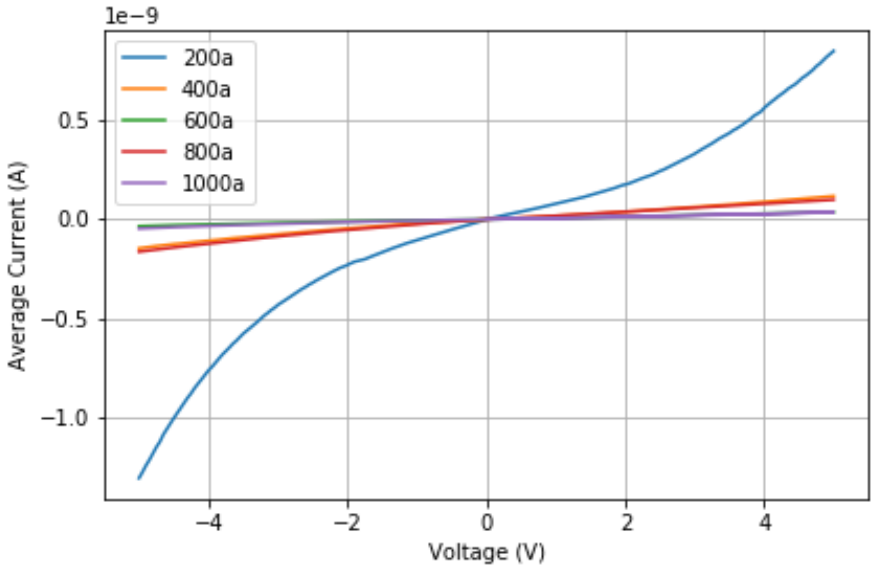

Figure 3.4: Average current response for films of different trials

3.2.4 Effect of ITO

In previous work in the literature, ZnO has been doped with Mn[24] via planetary ball milling. Although these materials have been studied together by sputtering[50], the effect of grinding ITO with ZnO has not been studied, and thus it was attempted in this work. $1.003g$ of ITO was mixed with $7.2341g$ of ZnO in $15mL$ of IPA for 10 minutes at 200rpm, similar to trial ZnO-IPA-1(see table 2.1). Films were also fabricated under similar conditions to facilitate meaningful comparison.

The addition of ITO resulted in visibly different electrical properties of the measured films. The I-V curve of the films tended to be more linear than the films ground without ITO, and were generally more repeatable, as evidenced from a sample shown in figure 3.5. This can be attributed to the conductive nature of ITO[47]. The current tended to saturate when the device was in the light, but as soon as it was removed, the current dropped on consecutive measurements at the same voltages.

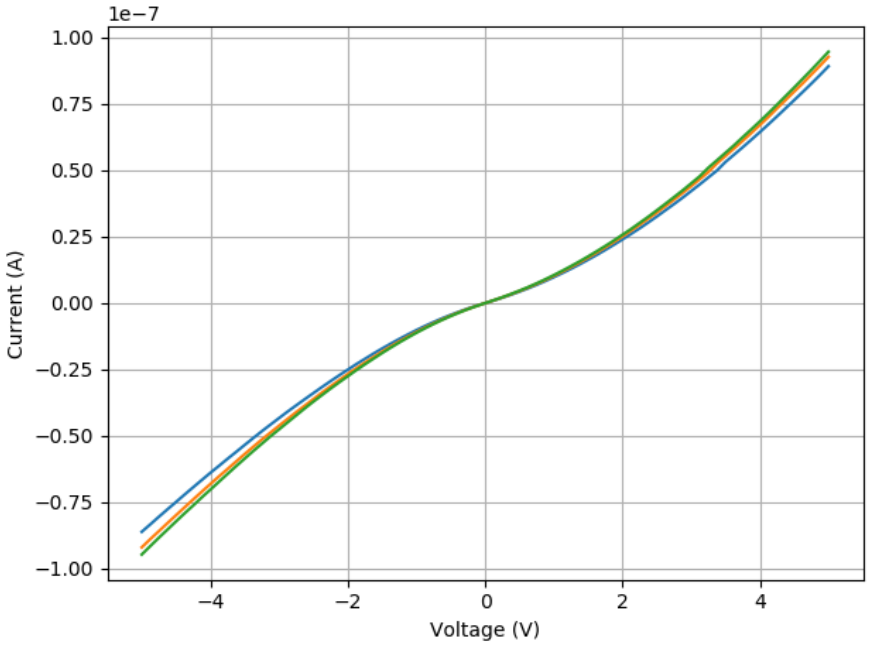

Figure 3.5: Current-voltage curve of a typical film of trial ZnO-ITO-IPA-1 under light

At first, four films of each were fabricated from vials 2 and 3 of this grinding trial (ZnO-ITO-IPA-1) from 3µL drops, and dried at 150℃ for 2 hours. Then silver electrodes were painted on and the films were dried for another 30 minutes at 100℃. The electrical characteristics of these set of films were measured after 3 days in air. The films showed interesting behaviour when measured in the dark as the I-V curve did not pass through the origin. This can perhaps be attributed to charge trapping from the passing of current, due to the addition of ITO nanoparticles. On continuing the changing of bias in a particular direction, the curve flattens out but there seems to be current flow even at zero applied bias. However, later investigations found that this behaviour is more likely an artifact resulting from the instrumentation at very low current values. Interestingly, this behaviour disappeared in the presence of light, as the I-V measurements of films under irradiation passed through the origin. This can be predicted by considering the same hypothesis, as light excites the electrons already present in the film to occupy and saturate the trap states. Thus there is no net intrinsic bias and the device behaves like a resistor from the start. It must be noted that the data is not enough to rule out a different hypothesis - that this is the effect of residual solvent or some other form of organic functionalization of the particles. Despite the cause, if this behaviour can be reliably reproduced, that is an indication that memristive devices can be fabricated by

mixing ITO and ZnO nanoparticles. Further experimentation and characterization is needed to reveal more information in this regard.

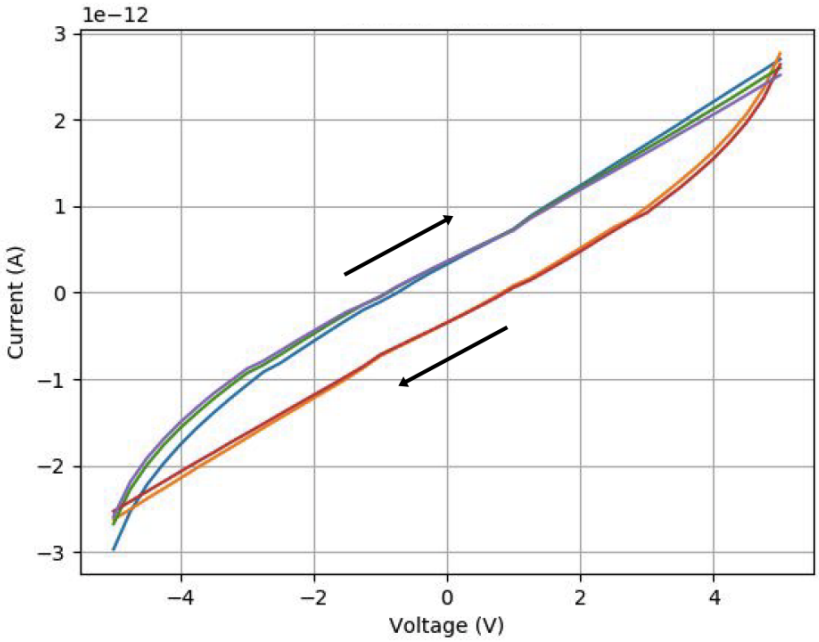

Figure 3.6: Artifacts in the cycled current-voltage curves of a film of ZnO-ITO-IPA-1

To compare the effect of adding ITO against pure ZnO, once again averaging a large number of measurements on films prepared under the same conditions is useful to account for variations in device dimensions. For the plot shown in figure 3.7, four drops of 3μL of each trial were casted onto glass slides after vigorous shaking and 60 seconds of sonication. Data from the second vial of the trials was used for the plot shown below. The films were initially annealed at 250℃ for two hours, after which the electrodes were painted on and the silver paint was dried at 200℃ for 20 minutes. Voltage sweeps of -5V to +5V were carried out to measure current response. All the films were measured in similar lighting conditions to avoid the effect of bias due to light.

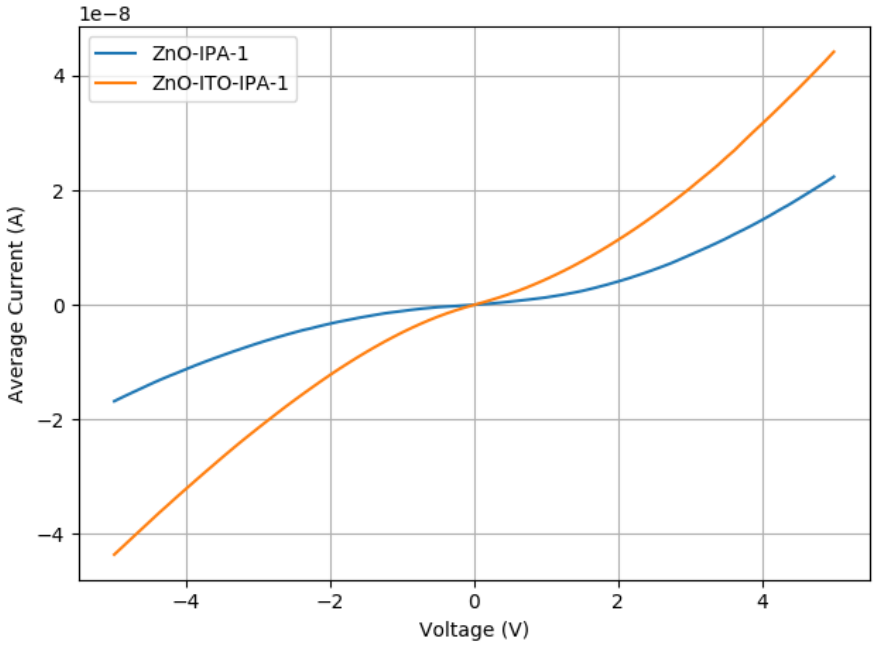

Figure 3.7: Average current response for films with and without ITO

3.3 Discussion

An I-V characteristic of one of the samples measured (film fabricated from grinding trial 400a) is presented in figure 3.8 below. It is visible that the measured curve is similar to the ideal I-V curve of figure1.18. This is a confirmation that the films form good contacts, and the current-voltage characteristic is as expected from a metal-semiconductor-metal junction. A sample curve from one of the measurements is presented below in figure 3.8, and it should be noted that all of the films of ZnO displayed a similar characteristic.

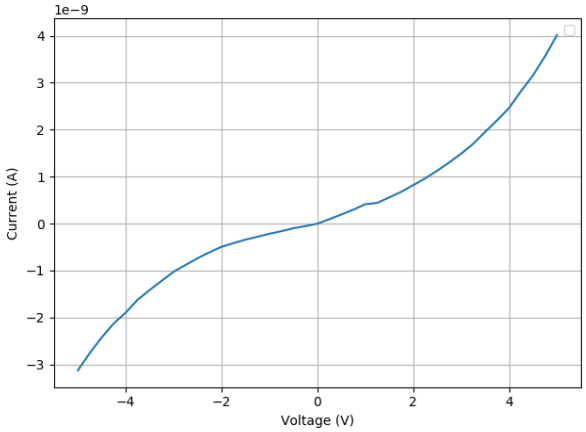

Figure 3.8: Current-voltage characteristic of a film of 400a

Since ZnO is a semiconductor, it will be affected by light of the appropriate wavelengths. Photons with enough energy can excite electrons from the valence band to the conduction band and thus enhance the current flow through the device. This effect has been used to create UV photodetectors with ZnO as the photocatalytic activity is strongly defined by various nanostructured properties[51]. Conceptually, the effect can be understood using the energy band diagram as shown in figure3.9. However, it is not necessary that the energy of the photons be equal or more than the bandgap to result in enhanced current on irradiation. This is due the presence of shallow and deep defect levels which ensure that the films display enhanced photoconductivity even when irradiated with photons in the visible wavelength. Further, it can be verified that the enhanced current is due to photoconductivity by noting the effect of increased irradiation intensity. Indeed it is found that higher intensity irradiation results in higher values of current for a given voltage. This effect can be observed across all the trials, irrespective of other factors. The effect of increased current due to photoconductivity was observed to be an immediate change. Removal of irradiation resulted in an initial sharp decrease in current followed by a gradual decrease in the current response over time. This validates the theory[31] presented in earlier sections that the excess electrons from excitement result in a net desorption of oxygen ions. Upon removal of irradiation, there is a reversal of this process, and there is a net increase in adsorbed oxygen over time, which leads to the continuous but decaying decrease in conductivity of the films. This hypothesis can be verified further by controlling the atmospheric environment of the films while they are being measured. This follows previoius studies where ZnO thin films been used for sensor applications[52], validating

planetary ball milling as a suitable synthesis technique for the active material.

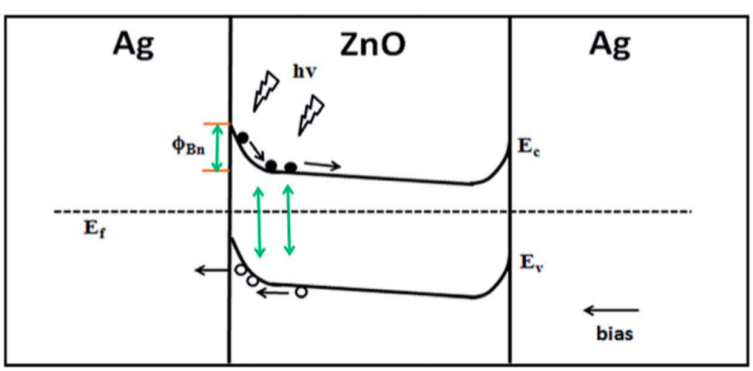

Figure 3.9: Energy band diagram of an Ag-ZnO-Ag UV photodetector [53]

Thermal treatment of the films also resulted in larger current response. Annealing has been known to increase the conductivity of ZnO nanoparticle thin films upon a subsequent return to room temperature[46]. This has been explained by an increase in the crystallinity resulting from the heat treatment, as surface corrosion products are re-converted to polycrystalline ZnO even at low temperatures of annealing. In the study just cited, Raman spectroscopy also confirmed the removal of residual organic species. Due to the high energies of ball milling, it is likely that the nanoparticles were coated with radicals from the organic solvent used in the grinding jar. While this is favourable for obtaining non-agglomerated dispersions, it is not favourable for obtaining higher conductivity as it means poor interparticle contacts throughout the films. Even though the films were annealed at temperatures higher than the boiling point of the solvent used (IPA), it was not enough to completely rid the films of the covalently attached organic species. It was hypothesized that annealing would affect the electrical properties of the films. Other than evaporating solvent, the heat also serves to facilitate better interparticle contact between the nanoparticles of ZnO as well as with the electrode[54]. The increased polycrystallinity of the nanoparticles would also mean less availability of dangling bonds on the surface and thus a decrease in the availibility of adsorption sites for atmospheric oxygen ions or hydrogen atoms. Finally, since very high temperature annealing was not performed, it is possible that the thermal energy resulted in an increase in the number of defects in the films by providing the energy needed for interstitial defects to form. This would also contribute to an increase in the conductivity that is observed due to the heat treatment.

Previous studies[24][41] have established the reduction in nanoparticle size of ZnO with the increase

in milling speed. The higher energy processes result in stronger impacts that fracture the particles to smaller sizes. Starting from unground nanoparticle films, a clear trend of increasing resistivity with increasing milling speeds was observed. This trend is also observed in the present work. As the volume of ground material used to fabricate the films was kept constant, there is an increase in the number of nanoparticles per thin film as the milling speed is increased. This would result in an increase in interparticle junctions and grain boundaries, which is a source of resistance[17]. In figure 3.11 below, the effect of grinding speed on films that have undergone the same fabrication process is visualised. It should also be noted that at higher speeds, the movement of the milling beads can enter a different regime. It is unclear exactly when this occurs, but needless to say there are many factors at play that affect the electrical properties of the zinc oxide nanoparticles after grinding. Further studies can help to determine the cause of these observations.

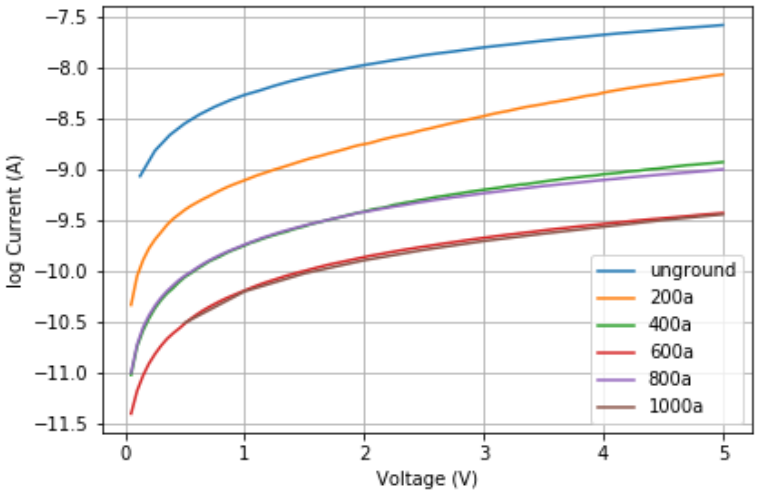

Figure 3.10: Semilog I-V plot of ZnO thin films

After grinding ZnO with ITO, the resultant slurry was observed to be uniform and did not separate over time. However, without adequate structural characterization techniques, it is not possible to provide a conclusive statement about whether or not doping takes place. The addition of ITO clearly affects the characteristics of the films, and since ITO is known to be an excellent conductor, it is no surprise that an increase in conductivity is observed. It is suggested that at least a small amount of doping took place because of the following observation - compared to pure ZnO that was grinded at the same parameters, the addition of ITO also resulted in films that were more sensitive to light irradiation. For a given

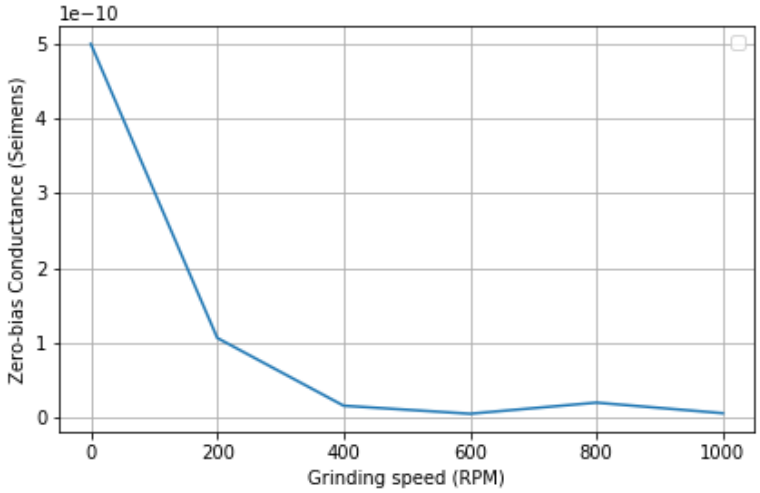

Figure 3.11: Variation of zero-bias conductance with grinding speed

baseline value of current measured in the dark, the films of the mixture of materials showed a larger increase in current when irradiated with the same intensity of light. The mechanism responsible for this comparative increase in sensitivity to light remains to be studied. As both the grinding trials (with and without ITO) were conducted with the same process parameters, the higher abundance of defect states in the one case must be additional defects introduced in the ZnO nanoparticles by the In or Sn atoms. While pure ZnO has been used to demonstrate memristive propertices previously [46][55][45], no prior literature was found that used the same mixture and fabrication technique as presented in this work.

3.4 Summary

Drop casting was used to fabricate thin films. They were then dried for different times at different temperatures and subsequently electrically characterized. The behaviour of the lateral structured two terminal devices was found to resemble back to back Schottky barrier diodes. The effect of various process parameters was analysed from the measured I-V data. Light was found to increase the current flow through the devices, and this can be attributed to photon-induced excitation of electrons to the conduction band from trap states. It was found that heating of the films generally resulted in increased conductivity. The effect of grinding speed was a net decrease in conductivity of the films up to a certain extent. With regards to material doping, mixing ITO clearly affects the electrical properties of the films, making them more conductive and ohmic.

Chapter 4

Conclusion

4.1 Future Work

This work can be extended in a number of directions depending on the intended applications and interest. In the domain of nanofabrication, the size limit of the nanoparticles attained by milling can be studied by a systematic study varying the grinding parameters such as speed and duration of grinding, size of the milling balls, the liquid medium used for grinding and process control agents, if any. As this project was more focused on electronic applications for ZnO, some avenues of further research in this domain are discussed below.

4.1.1 Characterization

While prior literature has been covered to consider possibilities of reactions taking place during milling, compositional and structural characterization of the resultant material was not carried out. This is an important step as it is a source of information to better understand the phenomenon observed. For measuring the particle size distribution after grinding, dynamic light scattering (DLS) measurements are suggested. Following film fabrication, atomic force microscopy can provide information about surface roughness and packing of the nanoparticle film. Pre- and post- annealing, compositional studies such as Fourier Transformed Infra-Red spectroscopy (FTIR) or UV-visible spectroscopy can be performed to accurately quantify the compositional changes if any, such as evaporation of solvent or coating species.

Scanning Electron Microscopy (SEM) images of the film would be essential in the case of mixed material grinding to ascertain whether the materials separate into different phases in the film. Photoluminescence (PL) studies could shed light on the distribution of defect states and how it changes after grinding and other process steps.

4.1.2 Device fabrication and structures

In this preliminary study, only lateral two terminal thin film devices were fabricated. Since the conductivity in ZnO thin films highly depends on adsorbate ions, this is very advantageous for optoelectronic applications such as photodetection. More area of the device is exposed, enhancing the sensitivity to the environment. However, the path taken by the current is very unpredictable and also variable. It is not known how much of the electron flow occurs through the bulk of the particles under the surface. If alternating current is used, the skin effect will also come into play. For more precise and electronic studies with controlled thickness, vertical devices can also be fabricated. These devices would have a sandwich structure with the electrodes at the top and bottom and the active material in the middle.

Electronic properties of the material such as resistivity can be more precisely studied with these devices and should offer more repeatable results. Given a standard vertical device structure, the change in these properties across differently treated/fabricated materials can also be studied, as discussed in the next section. If device fabrication methods such as thermal evaporation are used, the thickness of the films can be controlled very precisely and the active layer can possibly be made thin enough to exhibit quantum confinement.

Given a material with the right properties and fabrication methods such as lithography, the vertical structures can be advanced [15]. With higher precision and control, instead of depostion over a large area, thin strips of material can be deposited. Two such substrates can then be placed together perpendicular to each other to create a crossbar array. Further, fabrication of ZnO nanowires is also widely reported in literature for various applications [56][23][57]. Thus random nanowire networks can also be used to study the multi-level memory effects [37], if found to be present.

A new concept for memristive/resistive logic devices based on an active layer of ZnO nanorods has also been demonstrated [55] where the underlying method of controlling the logic device is modulation

of the angle of incident light. As shown in the figure 4.1, at a certain angle, the light beam path changes abruptly from refraction to reflection, resulting in a reversible change in behaviour of the device from memristive to resistive.

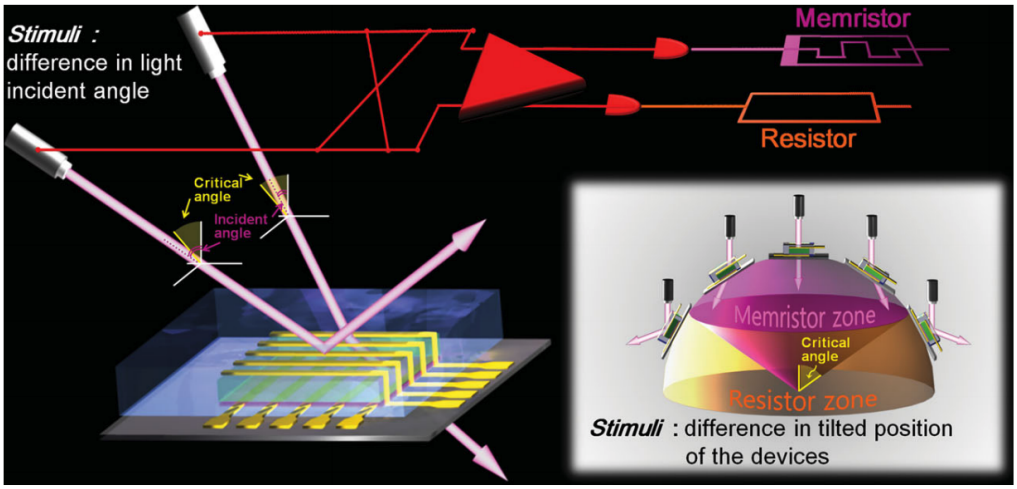

Figure 4.1: Schematic of Zinc Oxide device behaviour that is dependent on the angle of incident light [55]

An advantage of vertical device structures is that they can easily be extended to crossbar arrays. These networked devices are very efficient in their usage of space and materials, and are also comparatively easily to fabricate. They can be multiplexed easily and can be standardized to a shape that integrates onto other platforms such as FPGAs. However, lateral device structures are also relevant, and can be further explored with film fabrication techniques. Drop casting results in films with variations in dimensions, even if they are not immediately apparent to the naked eye. Thus future work can be done using thin film fabrication techniques that are more precise than drop casting, such as evaporation with masks, doctor blading, and stamp/template based techniques.

4.1.3 Composite and Dopant Materials

ZTO is a known high-performance semiconductor [30] that can also be used as a transparent conducting material [58]. ZnO can be n-doped up to high densities but it hard to achieve good p-doping in this wide-gap semiconductor [9]. Although most reports of fabricating doped thin films of ZnO use growth methods such as pulsed laser deposition or molecular beam epitaxy, doping using ball milling has also been reported in some cases [59]. The high impact energies of the milling process can allow for incorporating

changes in the lattice of the particles. Thus, grinding ZnO powder along with other materials that could dope it could result in different, interesting behaviours. Alternately, some materials (such as reduced graphene oxide nano-flakes) could also be mixed after the grinding process and then sonicated together before deposition or film fabrication.

Mixing known conductive materials such as graphene oxide [60], or carbon nanotubes [61] could be used to change the overall properties of the film. If they are grinded separately and then mixed, having small conductive particles among the less conductive ZnO particles could possibly allow for phenomena such as charge trapping. This would also result in electronic behaviour of the device that depends on its recent history. Memristive devices using ZnO have been demonstrated [55][45], and it could be valuable to pursue this avenue further.

Other than computational applications, making nanocomposites with ZnO could also lead to other desirable properties such as incorporation in polymer matrices for paint applications or into resins for making products where the active device and packaging is the same. Further, properties such as UV-sensitivity or chemical sensitivity induced via compositing materials can also be fine tuned by carefully varying the proportions of materials used. The planetary ball mill is very suited to such experiments of mixing materials into a homogenous nanocomposite.

4.2 Summary

Zinc oxide is a promising material for electronic applications due to its wide-bandgap electronic structure, and also due to being low cost and abundant in the earth's crust. The overall objective of this report was to explore the electronic properties of ZnO thin films formed via nano-grinding. Some interesting applications of ZnO include UV photodetectors as well as resistive memory. Planetary ball milling is a relatively inexpensive, reliable, straightforward, repeatable and tunable approach to reducing particle sizes of powder materials. In Chapter 2 we explored the process and parameters of the grinding, and fabrication and electrical characterization of the thin films. Chapter 3 presented the results of preliminary optical characterization of the films, and electrical characterization of two terminal devices. The I-V curves resembled that of metal-semiconductor-metal junctions. By repeatedly measuring the same films after putting them through heating cycles, the effect of thermal annealing on the electrical properties was

observed. The conductance was found to increase on additional annealing steps. The characteristics of the thin film devices were also compared across films made from materials ground at different speeds. In this case, the conductivity was found to decrease with increasing grinding speeds, and the rate of decrease was found to stagnate at higher rotation speeds. Finally, future avenues for research and development were suggested in this chapter, and potential applications discussed.

Bibliography

[1] International Technology Roadmap for Semiconductors (ITRS), "More Moore," *Itrs*, pp. 1–52, 2015.

[2] W. Han and Z. M. Wang, eds., *Toward Quantum FinFET*, vol. 17 of *Lecture Notes in Nanoscale Science and Technology*. Cham: Springer International Publishing, 2013.

[3] S. H. Jo, T. Chang, I. Ebong, B. B. Bhadviya, P. Mazumder, and W. Lu, "Nanoscale memristor device as synapse in neuromorphic systems," *Nano Letters*, vol. 10, no. 4, pp. 1297–1301, 2010.

[4] C. F. Burmeister and A. Kwade, "Process engineering with planetary ball mills," *Chemical Society Reviews*, vol. 42, no. 18, pp. 7660–7667, 2013.

[5] A. Stolle, T. Szuppa, S. E. Leonhardt, and B. Ondruschka, "Ball milling in organic synthesis: Solutions and challenges," *Chemical Society Reviews*, vol. 40, no. 5, pp. 2317–2329, 2011.

[6] W. Gao and Z. Li, "Nanostructures of zinc oxide," *International Journal of Nanotechnology*, vol. 6, no. 3-4, pp. 245–257, 2009.

[7] V. Srikant and D. R. Clarke, "On the optical band gap of zinc oxide," *Journal of Applied Physics*, vol. 83, no. 10, pp. 5447–5451, 1998.

[8] "CRC Handbook of Chemistry and Physics, 2009-2010, 90th ed. CRC Handbook of Chemistry and Physics, 2009-2010, 90th ed . Edited by David R. Lide , Editor-in-Chief, and W. M. "Mickey" Haynes , Associate Editor (National Institute of Standards and Technology,," *Journal of the American Chemical Society*, vol. 131, pp. 12862–12862, sep 2009.

[9] C. F. Klingshirn, "ZnO: Material, physics and applications," *ChemPhysChem*, vol. 8, no. 6, pp. 782–803, 2007.

[10] T. Yao, "Zinc Oxide," in *Encyclopedia of Materials: Science and Technology*, pp. 9883–9887, Elsevier, 2001.

[11] C. Klingshirn, J. Fallert, H. Zhou, J. Sartor, C. Thiele, F. Maier-Flaig, D. Schneider, and H. Kalt, "65 years of ZnO research - old and very recent results," *Physica Status Solidi (B) Basic Research*, vol. 247, no. 6, pp. 1424–1447, 2010.

[12] A. Janotti and C. G. Van De Walle, "Fundamentals of zinc oxide as a semiconductor," *Reports on Progress in Physics*, vol. 72, no. 12, 2009.

[13] K. Tang, S. L. Gu, J. D. Ye, S. M. Zhu, R. Zhang, and Y. D. Zheng, "Recent progress of the native defects and p-type doping of zinc oxide," *Chinese Physics B*, vol. 26, no. 4, pp. 0–23, 2017.

[14] L. Schmidt-Mende and J. L. MacManus-Driscoll, "ZnO - nanostructures, defects, and devices," *Materials Today*, vol. 10, no. 5, pp. 40–48, 2007.

[15] S. Lee, J. B. Park, M. J. Lee, and J. J. Boland, "Multilevel resistance in ZnO nanowire memristors enabled by hydrogen annealing treatment," *AIP Advances*, vol. 6, no. 12, 2016.

[16] C. Wöll, "The chemistry and physics of zinc oxide surfaces," *Progress in Surface Science*, vol. 82, no. 2-3, pp. 55–120, 2007.

[17] N. Salah, S. S. Habib, Z. H. Khan, A. Memic, A. Azam, E. Alarfaj, N. Zahed, and S. Al-Hamedi, "High-energy ball milling technique for ZnO nanoparticles as antibacterial material.," *International journal of nanomedicine*, vol. 6, pp. 863–869, 2011.

[18] D. Norton, Y. Heo, M. Ivill, K. Ip, S. Pearton, M. Chisholm, and T. Steiner, "ZnO: growth, doping & processing," *Materials Today*, vol. 7, pp. 34–40, jun 2004.

[19] M. Willander, O. Nur, Q. X. Zhao, L. L. Yang, M. Lorenz, B. Q. Cao, J. Ziga Pérez, C. Czekalla, G. Zimmermann, M. Grundmann, A. Bakin, A. Behrends, M. Al-Suleiman, A. El-Shaer, A. Che Mofor, B. Postels, A. Waag, N. Boukos, A. Travlos, H. S. Kwack, J. Guinard, and D. Le Si Dang, "Zinc oxide nanorod based photonic devices: Recent progress in growth, lightemitting diodes and lasers," *Nanotechnology*, vol. 20, no. 33, 2009.

[20] S. Dhara and P. K. Giri, "Quick single-step mechanosynthesis of ZnO nanorods and their optical characterization: milling time dependence," *Applied Nanoscience (Switzerland)*, vol. 1, no. 4, pp. 165–171, 2011.

[21] B. J. Norris, J. Anderson, J. F. Wager, and D. A. Keszler, "Spin-coated zinc oxide transparent transistors," *Journal of Physics D: Applied Physics*, vol. 36, no. 20, 2003.

[22] N. A. Shaari, S. M. Kasim, N. S. Sauki, and S. H. Herman, "The Effect of the Sol-gel Spincoating Deposition Technique on the Memristive Behaviour of ZnO-based Memristive Device," *IOP Conference Series: Materials Science and Engineering*, vol. 99, no. 1, 2015.

[23] J. Nause and S. Ganesan, "High-electron mobility transistor with zinc oxide," 2006.

[24] S. Sharma, S. S. Pande, and P. Swaminathan, "Top-down synthesis of zinc oxide based inks for inkjet printing," *RSC Advances*, vol. 7, no. 63, pp. 39411–39419, 2017.

[25] S. K. Hau, H. L. Yip, N. S. Baek, J. Zou, K. O'Malley, and A. K. Jen, "Air-stable inverted flexible polymer solar cells using zinc oxide nanoparticles as an electron selective layer," *Applied Physics Letters*, vol. 92, no. 25, pp. 2006–2009, 2008.

[26] M. A. Ibrahem, H. Y. Wei, M. H. Tsai, K. C. Ho, J. J. Shyue, and C. W. Chu, "Solution-processed zinc oxide nanoparticles as interlayer materials for inverted organic solar cells," *Solar Energy Materials and Solar Cells*, vol. 108, pp. 156–163, 2013.

[27] C. Xia, Z. Qiao, C. Feng, J. S. Kim, B. Wang, and B. Zhu, "Study on zinc oxide-based electrolytes in low-temperature solid oxide fuel cells," *Materials*, vol. 11, no. 1, 2017.

[28] M. Y. Soomro, S. Hussain, N. Bano, I. Hussain, O. Nur, and M. Willander, "Hybrid organic zinc oxide white-light-emitting diodes on disposable paper substrate," *Physica Status Solidi (A) Applications and Materials Science*, vol. 210, no. 8, pp. 1600–1605, 2013.

[29] K. Saoud, R. Alsoubaihi, N. Bensalah, T. Bora, M. Bertino, and J. Dutta, "Synthesis of supported silver nano-spheres on zinc oxide nanorods for visible light photocatalytic applications," *Materials Research Bulletin*, vol. 63, pp. 134–140, 2015.

[30] M. G. Kim, H. S. Kim, Y. G. Ha, J. He, M. G. Kanatzidis, A. Facchetti, and T. J. Marks, "High-performance solution-processed amorphous zinc-indium-tin oxide thin-film transistors," *Journal of the American Chemical Society*, vol. 132, no. 30, pp. 10352–10364, 2010.

[31] Y. Takahashi, M. Kanamori, A. Kondoh, H. Minoura, and Y. Ohya, "Photoconductivity of ultrathin zinc oxide films," *Japanese Journal of Applied Physics*, vol. 33, no. 12R, pp. 661–665, 1994.

[32] S. Liang, H. Sheng, Y. Liu, Z. Huo, Y. Lu, and H. Shen, "ZnO Schottky ultraviolet photodetectors," *Journal of Crystal Growth*, vol. 225, no. 2-4, pp. 110–113, 2001.

[33] Y. J. Hong, S. J. An, H. S. Jung, C. H. Lee, and G. C. Yi, "Position-controlled selective growth of ZnO nanorods on si substrates using facet-controlled GaN micropatterns," *Advanced Materials*, vol. 19, no. 24, pp. 4416–4419, 2007.

[34] R. Micheloni, L. Crippa, and A. Marelli, *Inside NAND Flash Memories*. Dordrecht: Springer Netherlands, 2010.

[35] X. Zhang, G. P. Zhao, H. Fangohr, J. P. Liu, W. X. Xia, J. Xia, and F. J. Morvan, "Skyrmion-skyrmion and skyrmion-edge repulsions in skyrmion-based racetrack memory," *Scientific Reports*, vol. 5, p. 7643, jul 2015.

[36] M. Circuit, "Memristor-The Circuit," *IEEE Transactions on Circuit Theory*, vol. c, no. 5, pp. 507–519, 1971.

[37] P. M. Sheridan, F. Cai, C. Du, W. Ma, Z. Zhang, and W. D. Lu, "Sparse coding with memristor networks," *Nature Nanotechnology*, vol. 12, no. 8, pp. 784–789, 2017.

[38] R. Kozma, R. E. Pino, and G. E. Pazienza, eds., *Advances in Neuromorphic Memristor Science and Applications*. Dordrecht: Springer Netherlands, 2012.

[39] C. Papadopoulos, *Solid-State Electronic Devices*. Undergraduate Lecture Notes in Physics, New York, NY: Springer New York, 2014.

[40] Y. Wan, Y. Li, Q. Wang, K. Zhang, and Y. Wu, "The relationship of surface roughness and work function of pure silver by numerical modeling," *International Journal of Electrochemical Science*, vol. 7, no. 6, pp. 5204–5216, 2012.

[41] R. Sapkota, J. Zou, S. Dawka, J. E. Bobak, and C. Papadopoulos, "Multi-functional thin film coatings formed via nanogrinding," *Applied Nanoscience (Switzerland)*, vol. 8, no. 6, pp. 1437–1444, 2018.

[42] D. L. Zhang, "Processing of advanced materials using high-energy mechanical milling," *Progress in Materials Science*, vol. 49, no. 3-4, pp. 537–560, 2004.

[43] A. Bruckmann, A. Krebs, and C. Bolm, "Organocatalytic reactions: Effects of ball milling, microwave and ultrasound irradiation," *Green Chemistry*, vol. 10, no. 11, pp. 1131–1141, 2008.

[44] H. Mio, J. Kano, F. Saito, and K. Kaneko, "Effects of rotational direction and rotation-to-revolution speed ratio in planetary ball milling," *Materials Science and Engineering A*, vol. 332, no. 1-2, pp. 75–80, 2002.

[45] W. Y. Chang, Y. C. Lai, T. B. Wu, S. F. Wang, F. Chen, and M. J. Tsai, "Unipolar resistive switching characteristics of ZnO thin films for nonvolatile memory applications," *Applied Physics Letters*, vol. 92, no. 2, pp. 2–5, 2008.

[46] S. Paul, P. G. Harris, C. Pal, A. K. Sharma, and A. K. Ray, "Low cost zinc oxide for memristors with high On-Off ratios," *Materials Letters*, vol. 130, pp. 40–42, 2014.

[47] M. Gross, A. Winnacker, and P. J. Wellmann, "Electrical, optical and morphological properties of nanoparticle indium-tin-oxide layers," *Thin Solid Films*, vol. 515, no. 24 SPEC. ISS., pp. 8567–8572, 2007.

[48] R. A. Gilstrap, C. J. Capozzi, C. G. Carson, R. A. Gerhardt, and C. J. Summers, "Synthesis of a nonagglomerated indium tin oxide nanoparticle dispersion," *Advanced Materials*, vol. 20, no. 21, pp. 4163–4166, 2008.

[49] K. Anand, S. Varghese, and T. Kurian, "Preparation of ultra-fine dispersions of zinc oxide by simple ball-milling: Optimization of process parameters," *Powder Technology*, vol. 271, pp. 187–192, 2015.

[50] T. Moriga, T. Okamoto, K. Hiruta, A. Fujiwara, I. Nakabayashi, and K. Tominaga, "Structures and physical properties of films deposited by simultaneous DC sputtering of ZnO and In2O3 or ITO targets," *Journal of Solid State Chemistry*, vol. 155, no. 2, pp. 312–319, 2000.

[51] Y. Zheng, L. Zheng, Y. Zhan, X. Lin, Q. Zheng, and K. Wei, "Ag/ZnO heterostructure nanocrystals: Synthesis, characterization, and photocatalysis," *Inorganic Chemistry*, vol. 46, no. 17, pp. 6980–6986, 2007.

[52] A. Pimentel, S. H. Ferreira, D. Nunes, T. Calmeiro, R. Martins, and E. Fortunato, "Microwave synthesized ZnO nanorod arrays for UV sensors: A seed layer annealing temperature study," *Materials*, vol. 9, no. 4, 2016.

[53] X. Zhang, Y. Qiu, D. Yang, B. Li, H. Zhang, and L. Hu, "Enhancing performance of Ag-ZnO-Ag UV photodetector by piezo-phototronic effect," *RSC Advances*, vol. 8, no. 28, pp. 15290–15296, 2018.

[54] K. Ellmer, "Resistivity of polycrystalline zinc oxide films: Current status and physical limit," *Journal of Physics D: Applied Physics*, vol. 34, no. 21, pp. 3097–3108, 2001.

[55] J. Park, S. Lee, J. Lee, and K. Yong, "A light incident angle switchable ZnO nanorod memristor: Reversible switching behavior between two non-volatile memory devices," *Advanced Materials*, vol. 25, no. 44, pp. 6423–6429, 2013.

[56] Z. L. Wang and J. Song, "Piezoelectric nanogenerators based on zinc oxide nanowire arrays," *Science*, vol. 312, no. 5771, pp. 242–246, 2006.

[57] T. K. Gupta, "Application of Zinc Oxide Varistors," *Journal of the American Ceramic Society*, vol. 73, no. 7, pp. 1817–1840, 1990.

[58] J. H. Ko, I. H. Kim, D. Kim, K. S. Lee, T. S. Lee, B. Cheong, and W. M. Kim, "Transparent and conducting Zn-Sn-O thin films prepared by combinatorial approach," *Applied Surface Science*, vol. 253, no. 18, pp. 7398–7403, 2007.

[59] O. Yamamoto, Y. Iida, and T. Sasamoto, "Change in Antibacterial Activity with Doping Amount of MnO2 in ZnO-MnO2 Solid Solution," *International Journal of Inorganic Materials*, vol. 2, pp. 451–454, 2000.

[60] J. I. Paredes, S. Villar-Rodil, A. Martínez-Alonso, and J. M. Tascón, "Graphene oxide dispersions in organic solvents," *Langmuir*, vol. 24, no. 19, pp. 10560–10564, 2008.

[61] S. S. S. A. Aziz, N. I. Harun, N. Salleh, S. A. Senawi, H. Azhan, S. N. H. Mohd Yusoff, Y. Mohd Amin, and R. Md Nor, "Mechanochemical synthesis of CNT/ZnO hybrid materials," *Materials Science Forum*, vol. 846, no. March, pp. 479–483, 2016.